

**Palaeoclimate constraints on a world with post-industrial warming of 2 degrees
and beyond**

Hubertus Fischer (*Climate and Environmental Physics, Physics Institute, and Oeschger Centre for
Climate Change Research, University of Bern, Bern, Switzerland*), **Katrin J. Meissner** (*Climate
Change Research Centre, University of New South Wales Sydney and ARC Centre of Excellence for
Climate System Science, Sydney, Australia*), **Alan C. Mix** (*College of Earth, Ocean, and
Atmospheric Sciences, Oregon State University, Corvallis, United States*), **Nerilie J. Abram**
(*Research School of Earth Sciences, The Australian National University and ARC Centre of
Excellence for Climate Extremes, Canberra, Australia*), **Jacqueline Austermann** (*Bullard
Laboratories, Department of Earth Sciences, University of Cambridge, Cambridge, United
Kingdom*), **Victor Brovkin** (*Max Planck Institute for Meteorology, Hamburg, Germany*), **Emilie
Capron** (*Centre for Ice and Climate, Niels Bohr Institute, University of Copenhagen, Copenhagen,
Denmark and British Antarctic Survey, Cambridge, United Kingdom*), **Daniele Colombaroli** (*Centre
for Quaternary Research (CQR), Department of Geography, Royal Holloway University of London
(RHUL), Egham, Surrey TW20 0EX, UK, Institute of Plant Sciences, Oeschger Centre for Climate
Change Research, University of Bern, Bern, Switzerland and Limnology Unit, Department of
Biology, Ghent University, Ghent, Belgium*), **Anne-Laure Daniau** (*Environnements et
Paléoenvironnements Océaniques et Continentaux, CNRS, Université de Bordeaux, Pessac, France*),
Kelsey A. Dyez (*Lamont-Doherty Earth Observatory, Columbia University, Palisades, United
States*), **Thomas Felis** (*MARUM - Center for Marine Environmental Sciences, University of Bremen,
Bremen, Germany*), **Sarah A. Finkelstein** (*Department of Earth Sciences, University of Toronto,
Toronto, Canada*), **Samuel L. Jaccard** (*Institute of Geological Sciences and Oeschger Centre for
Climate Change Research, University of Bern, Bern, Switzerland*), **Erin L. McClymont**
(*Department of Geography, Durham University, Durham, United Kingdom*), **Alessio Rovere**

26 *(MARUM - Center for Marine and Environmental Sciences, University of Bremen, and Leibniz*
27 *Center for Tropical Marine Ecology, Bremen, Germany), Johannes Sutter (Alfred Wegener*
28 *Institute, Helmholtz Centre for Polar and Marine Research, Bremerhaven, Germany), Eric W.*
29 **Wolff** *(Department of Earth Sciences, University of Cambridge, Cambridge, United Kingdom),*
30 **Stéphane Affolter** *(Climate and Environmental Physics, Physics Institute and Oeschger Centre for*
31 *Climate Change Research, University of Bern, Bern, Switzerland, International Foundation High*
32 *Altitude Research Stations Jungfrauoch and Gornergrat, Bern, Switzerland), Pepijn Bakker*
33 *(MARUM - Center for Marine and Environmental Sciences, University of Bremen, Bremen,*
34 *Germany), Juan Antonio Ballesteros-Cánovas (Institute for Environmental Sciences and Dendrolab,*
35 *Department of Earth Sciences, University of Geneva, Switzerland), Carlo Barbante (Institute for the*
36 *Dynamics of Environmental Processes - CNR, University Ca' Foscari of Venice, Venice, Italy),*
37 **Thibaut Caley** *(Environnements et Paléoenvironnements Océaniques et Continentaux, CNRS,*
38 *Université de Bordeaux, Pessac, France), Anders E. Carlson (College of Earth, Ocean, and*
39 *Atmospheric Sciences, Oregon State University, Corvallis, United States), Olga Churakova*
40 *(Sidorova) (Institute for Environmental Sciences, University of Geneva, Geneva, Switzerland,*
41 *Siberian Federal University, Institute of Ecology and Geography, Krasnoyarsk, Russia), Giuseppe*
42 **Cortese** *(GNS Science, Lower Hutt, New Zealand), Brian F. Cumming (Department of Biology,*
43 *Queen's University, Kingston, Canada), Basil A. S. Davis (Institute of Earth Surface Dynamics,*
44 *University of Lausanne, Lausanne, Switzerland), Anne de Vernal (Centre de recherche en*
45 *géochimie et géodynamique, Université du Québec à Montréal, Montréal, Canada), Julien Emile-*
46 **Geay** *(Department of Earth Sciences, University of Southern California, Los Angeles, United*
47 *States), Sherilyn C. Fritz (Department of Earth and Atmospheric Sciences, University of Nebraska-*
48 *Lincoln, Lincoln, USA), Paul Gierz (Alfred Wegener Institute, Helmholtz Centre for Polar and*
49 *Marine Research, Bremerhaven, Germany), Julia Gottschalk (Institute of Geological Sciences,*
50 *Oeschger Centre for Climate Change Research, University of Bern, Bern, Switzerland), Max D.*

51 **Holloway** (*Ice Dynamics and Paleoclimate, British Antarctic Survey, Cambridge, United Kingdom*),
52 **Fortunat Joos** (*Climate and Environmental Physics, Physics Institute, and Oeschger Centre for*
53 *Climate Change Research, University of Bern, Bern, Switzerland*), **Michal Kucera** (*MARUM -*
54 *Center for Marine and Environmental Sciences, University of Bremen, Bremen, Germany*), **Marie-**
55 **France Loutre** (*Past Global Changes (PAGES), Bern, Switzerland*), **Daniel J. Lunt** (*School of*
56 *Geographical Sciences and Cabot Institute, University of Bristol, Bristol, United Kingdom*),
57 **Katarzyna Marcisz** (*Laboratory of Wetland Ecology and Monitoring, Department of Biogeography*
58 *and Palaeoecology, Faculty of Geographical and Geological Sciences, Adam Mickiewicz University,*
59 *Poznań, Poland and Institute of Plant Sciences, Oeschger Centre for Climate Change Research,*
60 *University of Bern, Bern, Switzerland*), **Jennifer R. Marlon** (*School of Forestry and Environmental*
61 *Studies, Yale University, New Haven, United States*), **Philippe Martinez** (*Université de Bordeaux,*
62 *Pessac, France*), **Valerie Masson-Delmotte** (*Laboratoire des Sciences du Climat et de*
63 *l'Environnement, Gif-sur-Yvette cedex, France*), **Christoph Nehrbass-Ahles** (*Climate and*
64 *Environmental Physics, Physics Institute, and Oeschger Centre for Climate Change Research,*
65 *University of Bern, Bern, Switzerland*), **Bette L. Otto-Bliesner** (*Climate and Global Dynamics*
66 *Laboratory, National Center for Atmospheric Research, Boulder, United States*), **Christoph C.**
67 **Raible** (*Climate and Environmental Physics, Physics Institute, and Oeschger Centre for Climate*
68 *Change Research, University of Bern, Bern, Switzerland*), **Björg Risebrobakken** (*Uni Research*
69 *Climate, Bjerknes Centre for Climate Research, Bergen, Norway*), **María F. Sánchez Goñi** (*École*
70 *Pratique des Hautes Études, PSL Research University and Université de Bordeaux, Pessac, France*),
71 **Jennifer Saleem Arrigo** (*United States Global Change Research Program, National Coordination*
72 *Office, USA*), **Michael Sarnthein** (*Institute for Geosciences, University of Kiel, Kiel, Germany*),
73 **Jesper Sjolte** (*Quaternary Sciences, Department of Geology, Lund University, Lund, Sweden*),
74 **Thomas F. Stocker** (*Climate and Environmental Physics, Physics Institute, University of Bern,*
75 *Bern, Switzerland*), **Patricio A. Velasquez Álvarez** (*Physics Institute, University of Bern,*

76 Switzerland), **Willy Tinner** (*Institute of Plant Sciences, Oeschger Centre for Climate Change*
77 *Research, University of Bern, Bern, Switzerland*), **Paul J. Valdes** (*School of Geographical Sciences,*
78 *University of Bristol, United Kingdom*), **Hendrik Vogel** (*Institute of Geological Sciences, Oeschger*
79 *Centre for Climate Change Research, University of Bern, Bern, Switzerland*), **Heinz Wanner**
80 (*Oeschger Centre for Climate Change Research, University of Bern, Bern, Switzerland*), **Qing Yan**
81 (*Nansen-Zhu International Research Centre, Institute of Atmospheric Physics, Chinese Academy of*
82 *Sciences, Beijing, China*), **Zicheng Yu** (*Department of Earth and Environmental Sciences, Lehigh*
83 *University, Bethlehem, United States*), **Martin Ziegler** (*Department of Earth Sciences, Faculty of*
84 *Geosciences, Utrecht University, Utrecht, The Netherlands and Geological Institute, ETH Zürich,*
85 *Zürich, Switzerland*), **Liping Zhou** (*Laboratory for Earth Surface Processes, Department of*
86 *Geography, and Institute of Ocean Research, Peking University, Beijing, China*)
87

Abstract:

Over the past 3.5 million years, there have been several intervals when climate conditions were warmer than during the preindustrial Holocene. Although past intervals of warming were forced differently than future anthropogenic change, such periods can provide insights into potential future climate impacts and ecosystem feedbacks, especially over centennial to millennial timescales that are often not covered by climate model simulations. Our observation based synthesis of the understanding of past intervals with temperatures within the range of projected future warming suggests that there is a low risk of runaway greenhouse gas feedbacks for global warming of no more than 2°C. However, substantial regional environmental impacts can occur. A global average warming of 1-2°C with strong polar amplification has, in the past, been accompanied by significant shifts in climate zones and the spatial distribution of land and ocean ecosystems. Sustained warming at this level has also led to substantial reductions of the Greenland and Antarctic ice sheets, with sea-level increases of at least several meters on millennial time scales. Comparison of paleo observations with climate model results suggests that, due to the lack of certain feedback processes, model based climate projections may underestimate long-term warming in response to future radiative forcing by as much as a factor of two, and thus may also underestimate centennial to millennial-scale sea level rise.

1. Past warm intervals as benchmarks for future environmental changes

Depending on the choice of future carbon emission scenarios, projected global surface air temperature changes for the end of this century relative to preindustrial conditions (defined here as average conditions from 1850-1900 AD¹) range from 1.6°C (0.9°C to 2.4°C, 5-95% confidence interval, RCP2.6) to 4.3°C (3.2°C to 5.5°C, 5-95% confidence interval, RCP8.5²). Models project substantially higher warming at high latitudes with Arctic temperature changes being amplified in simulations by a factor of 2 to 3, implying future warming of ~3°C (RCP2.6) to ~12°C (RCP8.5) in these regions. Moreover, in most areas, the warming is projected to be greater over land than over the ocean.

Even if future emissions are reduced, warming will continue beyond 2100 for centuries or even millennia because of the long-term feedbacks related to ice loss and the carbon cycle^{3,4}. Given concern about these impacts, the Paris agreement proposes reducing emissions to limit global average warming to below 2°C and pursue efforts to limit it to 1.5°C, effectively defining a climate “defense line”⁵. Although this guardrail concept is useful, it is appropriate to ask whether the global limits proposed in the Paris COP-21 Climate Agreement really constitute a safe operating space for humanity⁶ on our complex planet.

Many state-of-the-art climate models may underestimate both rates and extents of changes observed in paleo data⁷. Models are calibrated based on recent observations, simplifying some processes (e.g., the representation of clouds and aerosols) or neglecting processes important on long timescales under significantly warmer boundary conditions (e.g., ice sheet dynamics or carbon cycle feedbacks). This lack of potentially important feedback mechanisms in climate models underscores the importance of exploring warm climate intervals in Earth’s history. Understanding these past intervals may

illuminate feedback mechanisms that set long-term climate and Earth System sensitivity, enabling an assessment of possible impacts of warming on physical, biological, chemical, and ecosystem services upon which humanity depends.

Examples of such warmer conditions with essentially modern geographies can be found in Figure 1 during the Holocene Thermal Maximum (HTM) and the Last Interglacial (LIG; ~129-116 kyr before present (BP), where present is defined as 1950). Here, the HTM is broadly defined as a period of generally warmer conditions in the time range 11-5 kyr BP, which, however, were not synchronous in their spatio-temporal expression. The LIG can also be compared to the warmer peak interglacial Marine Isotope Stage (MIS) 11.3 (~410-400 kyr BP) where climate reconstructions exist. Note that these times of peak warmth were associated with different orbital parameters, thus different spatial and seasonal distribution of solar insolation, while their greenhouse concentrations were close to preindustrial levels and their temperatures, although within the projected range of anthropogenic warming for the near future, have been controlled by a different blend of forcing mechanisms (see Section 2). Accordingly, past interglacials can be thought of as a series of natural experiments characterized by different combinations of climate boundary conditions⁸. Although they are not strict analogs for future warming, these past warm intervals do illustrate the regional climate and environmental response that may be triggered in the future, and thus remain useful as an observational constraint on projections of future impacts.

The HTM is amenable to detailed reconstruction based on availability of data and more refined approaches to chronology, but the older interglacial intervals illustrate greater warming and impacts. To examine past climates with greenhouse gas concentrations of >450 ppm (as expected for the RCP2.6), we must look farther back in time, to at least 3 Myr BP (Mid Pliocene Warm Period, MPWP, 3.3-3.0 Ma) when atmospheric CO₂ was between 300 and 450 ppm⁹ (Figure 1) and warm

conditions lasted long enough to approach equilibrium. Older intervals, such as the Early Eocene Climatic Optimum (EECO, ~53-51 Ma) offer an opportunity to study extremely high-CO₂ scenarios (900-1900 ppm) that are comparable with the fossil-fuel intensive RCP 8.5² scenario¹⁰ (>1200 ppm), however, these older intervals had continental configurations significantly different from today.

Paleo evidence over the last 2000 yr and during the Last Glacial Maximum (LGM) was discussed in detail in the 5th Assessment Report of the Intergovernmental Panel for Climate Change (IPCC)². Here we focus on the climate system responses during the three best-documented warm intervals HTM, LIG, and MPWP (Figure 1) and address spatial patterns of environmental changes and the forcing leading to them. Observations on the spatial temperature expression of these warm periods and their forcing are presented in Box 1, which also includes a discussion of the limitations of these time intervals as first-order analogs for future global and regional warming. Paleo evidence on the Earth System response to these warmer conditions is reviewed in Section 2 (summarized in Figure 3). Section 3 discusses potential feedbacks and thresholds in the climate system in light of the paleo record and their implications for future warming impacts. Based on the paleo evidence on climate, sea level and past CO₂ in warm intervals we assess the long-term Earth System Sensitivity (ESS)¹¹ as imprinted in the paleo record in Box 2 and draw conclusions on limitations of current climate models to predict the long-term (millennial) change in Earth's climate. Given the different continental configuration, we do not assess regional changes for the EECO in Section 2. We limit our analysis of the EECO to the issue of ESS in Box 2 based on available paleodata and published model experiments where we account for the global effects of changing distribution of landmasses at that time.

2. Earth System responses during warm intervals

2.1. Continental ice sheets and changes in sea-level

Although alpine glaciers, parts of the Greenland Ice Sheet (GIS) and some sectors of Antarctica may have had less ice during the HTM than today^{12,13}, sea-level was still ~26 m (9 kyr BP) to ~2 m (5 kyr BP) lower than present¹⁴ implying the presence (but ongoing melting) of remnants of the glacial maximum continental ice sheets. Greenland ice retracted to its minimum extent between 5 and 3 kyr BP, perhaps as a slow response to HTM warming¹⁵.

Global sea level reconstructions of 6-9 m higher than present during the LIG (and at least that for MIS11.3) require a substantial retreat of at least one of the Greenland and Antarctic ice sheets, but likely a significant reduction of both, relative to their current volumes¹⁶. During the LIG, the marine-terminating ice sheet in southern and central Greenland retreated to terrestrial margins¹⁷. While latest ice sheet and climate model simulations allow for a substantial retreat of the West Antarctic Ice Sheet (WAIS) and potentially parts of East Antarctica^{18,19}, direct observational evidence is still lacking. The GIS was also significantly reduced during MIS 11.3 peak warming with only a remnant ice cap in northern Greenland²⁰. Cosmogenic exposure dating of subglacial materials under Summit, Greenland, suggest loss of part of the GIS during some warm intervals of the Pleistocene²¹.

Ice sheets existed in Greenland and Antarctica during the MPWP, but their configuration is uncertain^{18,22}. A sea-level rise of 6 m or more implies substantially less global ice than present (upper limit poorly constrained) during the MPWP¹⁶, and this calls for a significant shrinkage of the GIS and/or AIS. Model results suggest a significantly reduced GIS²³, while geological data show evidence of West Antarctic deglaciation²⁴ and potentially also over the Wilkes subglacial basin in East Antarctica²⁵.

2.2. Sea ice

Qualitative reconstructions of sea ice extent and concentrations suggest reduced sea ice extent during past warm intervals both in the Arctic and around Antarctica^{26,27}. However, even during the LIG, with strongly elevated summer insolation, sea ice existed in the central Arctic Ocean during summer, whereas sea ice was significantly reduced along the Barents Sea continental margin and potentially other shelf seas²⁸. Ice core evidence for the LIG has been interpreted as suggesting that multi-year sea ice around Greenland was reduced, but winter sea ice cover was not greatly changed²⁹. In the Southern Ocean, reconciliation of climate model output with warming evidence from Antarctic ice cores suggests that Antarctic winter sea ice was reduced by >50 % at the onset of the LIG³⁰. However, although this reconstruction is consistent with a compilation of Southern Ocean sea ice proxy data, most published marine core sites are situated too far north for independent verification³⁰.

Based on limited observational evidence, generally reduced summer sea ice cover in the Arctic Basin has been reconstructed during the MPWP²³ and biomarkers at the Iceland Plateau indicate seasonal sea ice cover with occasional ice-free intervals. During this warm interval the East Greenland Current may have transported sea ice into the Iceland Sea and/or brought cooler and fresher waters favoring local sea ice formation³¹.

2.3. Marine plankton ecosystem changes

Warmer ocean temperatures influenced marine ecosystems. The HTM warming was regionally diachronous and therefore did not leave a globally consistent fingerprint on the surface layer plankton habitat³². There is nevertheless abundant evidence for changes in productivity, such as in the North Pacific, where early Holocene warming appears to have promoted diatom blooms and enhanced export production in warmer, more stratified surface waters³³.

A reorganization of ocean productivity was also documented during the LIG, with evidence for increased frequency and poleward expansion of coccolithophore blooms³⁴ and higher export production in the Antarctic Zone of the Southern Ocean^{35,36}. Strongly increased export production is also found in the Southern Ocean during the MPWP³⁷. The impacts of these changes on higher trophic levels and benthic ecosystems remain unexplored, except in the climatically sensitive marginal seas. Here, circulation changes during past warm intervals led to local extinctions and community reorganization in marine ecosystems³⁸, with a stronger response to LIG climate forcing than in the Holocene.

Whereas HTM and LIG marine communities are good compositional and taxonomic analogs to the present, MPWP marine ecosystems differ due to substantial species turnover (extinctions and originations)³⁹. In some groups of plankton, such as in planktonic foraminifera, enough extant species existed in the MPWP to judge general ecosystem shifts⁴⁰. Data from these groups indicate that poleward displacement of mid and high-latitude marine plankton during the MPWP was stronger than during the LIG, but the diversity-temperature relationship remained similar and comparable to the present⁴¹. Thus, oceanic marine plankton responded to warming with range shifts rather than by disruption of community structure.

2.4. Vegetation and climate on land

Extensive proxy data is available from all continents showing large changes in vegetation and shifts in moisture regimes, indicating that the HTM was complex and temporally variable. For example, major HTM changes in vegetation are marked by greening of the Sahara⁴², whereas in other regions, including the Northern Great Plains of North America, aridity increased and expanded east into the boreal biome⁴³. Many regions experienced a climate driven poleward extension of their biome boundaries with similar altitudinal vegetation expansions by a few hundred meters⁴⁴. The tundra and

tundra-forest boundary in eastern North America, Fennoscandia and Central Siberia shifted northward (by ~200 km), while forest shifted southward in eastern Canada (by ~200 km)⁴⁵.

During the LIG, tundra vegetation⁴⁶ contracted, the Sahara desert vanished⁴⁷, and boreal forest vegetation⁴⁸ and Savanna⁴⁷ expanded. Temperate taxa (hazelnut, oak, elm) were found north of their current distribution in southern Finland⁴⁹. In Siberia, birch and alder shrubs dominated vegetation compared to herb-dominated tundra at present⁵⁰. Southwestern Africa was marked by expansion of nama-karoo and fine-leaved savanna⁵¹.

In the MPWP, temperate and boreal vegetation zones shifted poleward (for example in East Asia and Scandinavia⁵²). Tropical savannas and forests expanded, while deserts contracted²³.

3. Amplification and thresholds - paleo lessons for the future

Understanding potential amplification effects and nonlinear responses in climate and environmental systems is essential, as they have substantial environmental and economic consequences⁵³. Many potential amplification effects are outside of historical human experience, so paleo data may help understand these processes.

3.1. Carbon cycle feedbacks

Radiative forcing over the last 800,000 years by the atmospheric greenhouse gases CO₂, CH₄ and N₂O was often lower but rarely higher than preindustrial values⁵⁴ and also greenhouse gas rise rates in past warm periods were much slower. Over the period 1987-2016, global annual greenhouse gas concentrations rose on average by 19 ppm/decade for CO₂ (with generally increasing rise rates over this 30 yr interval), by 57 ppb/decade for CH₄ and by 8 ppb/decade for N₂O (all data from

<https://www.esrl.noaa.gov/gmd/>), while during the last deglaciation, high-resolution ice core data (WAIS Divide and Taylor Glacier, Antarctica) reveal maximum natural rise rates up to a factor of 10 slower (~ 2.3 ppm/decade for CO_2 , ~ 21 ppb/decade for CH_4 , and 0.9 ppb/decade for N_2O ⁵⁴⁻⁵⁶). While these natural variations in greenhouse gas forcing represent a substantial contribution to glacial-interglacial climate variations, the climate mechanisms that drive changes in the carbon cycle and the associated climate feedbacks remain a matter of debate.

Analyses of last millennium CO_2 and northern hemisphere temperature variability suggest a warming-driven net CO_2 release from the land biosphere ($2 - 20$ ppm / $^\circ\text{C}$) on decadal-to-centennial scales^{57,58}. During short-term warming events in preindustrial times (when CO_2 was rather constant), net release of land carbon due to enhanced respiration of soil and biomass appears to compensate plant growth associated with fertilization effects by higher temperatures. A similar short-term response can be expected for future regional warming.

Peat accumulation rate is positively correlated with summer temperature⁵⁹, but is a relatively slow process. Peat reservoirs have gradually increased over the Holocene, resulting in long-term sequestration of carbon⁶⁰. HTM rates for net carbon uptake by northern peatlands were clearly higher than those for the cooler late Holocene^{61,62} as a result of rapid peatland inception and peat growth during times of ice sheet retreat and strong seasonality.

While peatlands were present during the LIG⁶³, the preserved record is fragmentary so the magnitude of LIG peat carbon storages is not well constrained. During the Pliocene (and MIS 11.3), peats were likely abundant but there are only a few dated peat deposits of this age (for instance German and Polish lignite⁶⁴). Boreal-type forested peatlands with thick peat accumulations may have accumulated over $>50,000$ years in response to warmer climates during the Pliocene⁶⁵.

305

306 Based on these paleo-environmental analogs, peatlands will likely expand in a 2°C warmer world on
307 centennial to millennial time scales, although the size of this sink is difficult to estimate based on the
308 paleo record alone and the net carbon source or sink may depend on the rate of warming and
309 moisture conditions. If warming is fast (decadal-to-centennial) carbon may be released via
310 respiration faster than it can accumulate via peat growth. If warming is slower (centennial-to-
311 millennial) continued peat growth may outstrip respiratory losses, yielding a net carbon sink.

312

313 Widespread permafrost thaw and enhanced fire frequency and/or severity could counteract carbon
314 sink effects of long-term peat growth⁶⁶. Today, about 1330-1580 gigatons of carbon (GtC) are stored
315 in perennial frozen ground, of which ~1000 GtC (more than the modern atmospheric carbon
316 inventory) are located in the upper 0-3 m of soil. This frozen carbon is susceptible to a thawing of
317 the upper permafrost layer under future warming⁶⁷ and risks of the related carbon release can be
318 assessed in ice core gas records. Although detailed data are limited, the observed variation of CO₂
319 and CH₄ in ice core records suggests that the risk of a sustained release of permafrost carbon is small
320 if warming can be limited to the modest high-latitude warming encountered during past interglacial
321 periods⁶⁸. Apart from short-lived positive excursions observed at the onset of many interglacials,
322 atmospheric CH₄ and CO₂ concentrations in the ice record^{69,70} were not significantly elevated in past
323 interglacials, in which the Arctic was significantly warmer than during preindustrial times⁵⁰.
324 Accordingly, the additional CO₂ and CH₄ releases at the onset of interglacials (if they were related to
325 permafrost warming⁷¹), were not sufficient or long enough to drive a long-term “runaway”
326 greenhouse-warming that outpaces negative feedback effects. If future warming is much greater than
327 that observed for past interglacials, release of carbon from permafrost remains a serious concern that
328 cannot be assessed based on the paleo evidence presented here.

329

A release of CH₄ from marine hydrates during climate warming as suggested from marine sediment records⁷² cannot be confirmed. Isotopic analysis of CH₄ preserved in ice cores suggests that gas hydrates did not contribute substantially to variations in atmospheric CH₄ during rapid warming events in the glacial and deglacial^{73,74}. This may suggest that long-term CH₄ releases are also unlikely to occur in future warming, as long as the magnitudes and rates of warming are limited to the range observed in the geologic record of past warm intervals.

Based on the evidence summarized above, the risk of future massive terrestrial CH₄ or CO₂ releases that may lead to a runaway greenhouse gas effect under modest warming scenarios of RCP2.6 appears to be limited. However, the amount of carbon released from permafrost as CO₂ may amount to up to 100 GtC⁷⁵ and has to be accounted for when implementing policies for future allowable anthropogenic carbon emissions. We cannot rule out net release of land carbon if future warming is significantly faster or more extensive than observed during past interglacials. Furthermore, past increases in CO₂ were mostly driven by changes in the physical and biological pumps in the ocean and - on long time scales - through interactions between ocean and sediments and the weathering cycle. The reconstruction of ocean carbon reservoirs during past warm episodes remains a challenge, and the risk of significant reductions of ocean CO₂ uptake or disturbances in the AMOC in the future with feedbacks on the carbon cycle are not well constrained.

3.2. Thresholds for ice sheet melting

Models of the GIS suggest extensive and effectively irreversible deglaciation above a certain temperature threshold, but the threshold is model dependent^{76,77}. Marine records of southern GIS sediment discharge and extent suggest the GIS was substantially smaller than present during three out of the last five interglacials⁷⁸ with near complete deglaciation of southern Greenland occurring

during MIS 11.3^{20,79}. This suggests that the threshold for southern GIS deglaciation is already passed for the polar temperature amplification signal associated with a persistent global warming by 2°C, i.e., within the range of the Paris Agreement (see Figure 2). Concentrations of cosmogenic radionuclides in bedrock at the base of Summit Greenland have been interpreted to suggest multiple periods of exposure of the western GIS during the last million years²¹. In contrast, the age of the basal ice at Summit Greenland suggests a persistent northern Greenland ice dome at least for the last million years⁷⁹. Vice versa, the southern Greenland ice dome existed during the LIG but melted at some time before 400 kyr BP⁷⁹. Marine records suggest the persistence of ice in eastern Greenland for at least the last 3 million years⁸⁰, which would imply different temperature thresholds for deglaciation of different portions of the GIS.

The WAIS was appreciated by AR5² and previous assessments as possessing an unstable marine-based geometry, but the thresholds at which strong positive feedbacks would be triggered were unknown, and models failed to reproduce past sea-level contributions². Several lines of observational evidence suggest episodes of major retreat of marine WAIS sectors^{81,82}. Marine-based sectors of the East Antarctic Ice Sheet (EAIS) are now known to be at similar risk of collapse as those of the WAIS^{25,83}. The main indicator for a substantial AIS contribution to global sea-level rise in past interglacials remains the sea-level proxy record¹⁶. The survival of parts of the GIS in the LIG requires a significant retreat of at least part of the AIS. Pliocene reconstructions of sea-level highstands require a substantial contribution of both the WAIS and EAIS but are subject to major uncertainties¹⁶.

Since AR5, model simulations are now more consistent with prior theory and sea-level constraints^{18,19,84}. Ice-sheet model simulations suggest that marine ice-sheet collapse can be triggered in sectors of the EAIS and WAIS for a local sub-surface ocean warming of +1-4°C^{18,19,84}. However,

thresholds for Antarctic marine ice-sheet collapse vary considerably between models and their parameterizations of ice-shelf mass balance and ice dynamics^{18,19,84}. While some models predict that Antarctica is now more sensitive than the literature assessed in AR5², the current geological record^{85,86} and modeling evidence are not sufficient to rule out or confirm tipping points for individual Antarctic sectors within the 1.5-2°C global warming range.

Of special societal relevance is also the rate of sea level increase. Sea-level rise has accelerated over the last century from 1.2 ± 0.2 mm/yr between 1901 and 1990 (largely due to thermosteric effects) to 3.0 ± 0.7 mm/yr over the last two decades as net melting of glaciers and ice sheets has increased⁸⁷. Records of paleo sea level rise rates expand our view into times when the melting response of the GIS and AIS may have been much larger than today. Sea-level changes within the LIG were likely between 3 and 7 mm/yr (1000-year average), with a 5% probability of >11 mm/yr⁸⁸. For example, exposed fossil coral reefs from Western Australia⁸⁹ suggest that, after a period of eustatic sea-level stability (127 to 120 kyr BP), sea-level rose quite quickly from 2.5 to nearly 8.5 meters in less than 1 kyr (i.e., 6 mm/yr). Indirect evidence for sea level rise from Red Sea isotopic measurements within the LIG allows rise rates as high as 16 mm/yr⁹⁰. All of these estimates are uncertain for both level and chronology and are subject to regional isostatic effects but multimeter-scale sea level oscillations within the Last Interglacial cannot be excluded¹⁶. They highlight the possibility that future sea level rise may be significantly faster than historical experience as also suggested in recent satellite altimeter data⁹¹.

3.3 Response of land ecosystems

The paleo record suggests sensitivity of forest ecosystems, specifically in ecotone positions, to moderate warming (1-2°C) at the decadal-to-centennial scale^{92,93}, with tipping points reached in

regions where moisture availability will go below critical ecophysiology levels for trees⁹⁴. At higher latitudes and in mountain ranges increased temperatures will promote forest expansion into tundra⁹⁵. Such northward shifts of boreal ecosystems will be counterbalanced by forest die-back in areas where increased drought will instead favor open woodlands or steppe⁹⁶.

Evidence from the HTM suggests that cool-temperate and warm-temperate (or subtropical) forests may collapse in response to climate warming of 1-2°C, if moisture thresholds are reached⁹⁷, and flammable, drought-adapted vegetation will rapidly replace late-successional evergreen vegetation in Mediterranean areas⁹⁸.

Substantial and irreversible changes are also expected for tropical forests, with large tree mortality occurring where peripheral areas of rainforest will turn into self-stabilizing, fire-dominated savanna⁹⁹. The green Sahara-desert transition that occurred at the end of the African Humid Period¹⁰⁰ implies that a warmer climate may cross the threshold to open, fire-maintained savanna and grassland ecosystems. Such rainfall thresholds are more easily reached with deforestation, and imply increased flammability, reduced tree reestablishment, and rapid runaway change toward treeless landscapes⁹⁹. Opposed to carbon reduction in tropical forests is fuel buildup in subtropical regions under increasing rainfall scenarios², implying that critical transitions will be spatially complex, depending on the position along moisture gradients^{96,99}.

4. Conclusions

Past warmer worlds were caused by different forcings, which limits the applicability of our findings to future climate change. Nevertheless we can conclude that even for a 2°C (and potentially 1.5°C) global warming - as targeted in the Paris Agreement¹⁰¹ - significant impacts on the Earth System are to be expected. Terrestrial and aquatic ecosystems will spatially reorganize to adapt to warmer conditions as they did in the past (e.g. HTM, LIG). However, human interferences other than climate

change, such as pollution, land-use, hunting/fishing and overconsumption, appear to have a much larger influence on species extinction and diversity loss¹⁰² than climate warming.

The risk of amplification such as runaway greenhouse gas feedbacks appears - based on the paleo record - to be small under the modest warming of RCP2.6. From this perspective, staying in a range of warming experienced during the past interglacial periods is appropriate to limit risks and impacts of climate change¹⁰¹. Although these findings support the 2°C global warming target of the Paris Agreement, more rapid or extensive warming in scenarios such as RCP8.5 would be outside the experience provided by past interglacial periods reviewed here. Such a pathway into conditions without well-studied precedent would be inherently risky for human society and sustainable development.

However, even a warming of 1.5-2°C is sufficient to trigger substantial long-term melting of ice in Greenland and Antarctica and sea-level rise that may last for millennia. For instance, the LIG and Marine Isotopic Stage 11.3 were characterized by prolonged warmer-than-present-day conditions in high latitudes, leading to melting of parts of Greenland and Antarctica. This ice sheet melt contributed to a more than 6 m sea-level rise compared to preindustrial¹⁶ on time scales of millennia and caused significantly higher rates of sea level rise compared to those of the last decades.

Comparison of paleo data and model estimates of long-term (multi-centennial to millennial) warming in response to CO₂ (see Box 2) suggests that models may underestimate observed polar amplification and global mean temperatures of past warm climate states by up to a factor of two on millennial time scales. Despite the significant uncertainties in climate and CO₂ reconstructions for many of the past warm intervals, this underestimation is likely because the models lack or potentially simplify key processes such as interactive ice sheets, cloud processes and biogeochemical feedbacks

that impact long-term Earth System Sensitivity. Again, this implies that long-term sea-level rise and regional and global warming may be significantly more severe than state-of-the-art climate models project.

Knowledge gaps remain for all periods and all processes, including the reconstructions of past CO₂ concentration, air and ocean temperatures, and ecosystem responses, but also for extreme events, and changes in variability (see supplementary text). It will be important to increase our understanding of cloud and aerosol physics, to improve the representation of cryosphere-climate and biogeochemical Earth System feedbacks in climate models used for long-term projections, and to refine paleo reconstructions as a key constraint for modeled climate sensitivity. In spite of existing uncertainties, our review of observed paleo data and models associated with known warmer climates of the past underscores the importance of limiting the rate and extent of warming to that of past interglacial warm intervals to reduce impacts such as food and ecosystem disruptions, loss of ice, and the inundation of vast coastal areas where much of the world's population and infrastructure resides.

Data availability: All data and model results used in this review paper are from published literature (see references provided in the main text and the supplementary tables).

472 Box 1 - Global and regional temperature changes in past warm intervals

473 The HTM surface warming relative to preindustrial conditions was on average $<1^{\circ}\text{C}^{107}$ and is mostly
474 expressed in northern-hemisphere proxies sensitive to the warm season. Although some regional
475 studies define the HTM narrowly as older than 8.2 kyr BP, here we take a broad definition of ~11-5
476 kyr BP. We exclude the 8.2 kyr cold event in the North Atlantic region, which is thought to have
477 been caused by a freshwater disturbance¹¹¹ in the North Atlantic and subsequent weakening of the
478 Atlantic Meridional Overturning Circulation (AMOC) and is likely not representative for a global
479 warming response expected for the end of this century.

480

481 The HTM was a complex series of events in which warming occurred while ice cover and sea-level
482 had not reached postglacial equilibrium and continental ice sheets in North America and Scandinavia
483 were still retreating. This complexity of residual ice cover makes it likely that HTM warming was
484 regional, rather than global, and its peak warmth, thus, had different timing in different locations¹⁰.
485 Ice core data show that radiative forcing due to greenhouse gases during the HTM was slightly lower
486 than preindustrial values¹¹². Compared to preindustrial conditions, the HTM orbital configuration
487 featured greatly enhanced summer insolation in high northern latitudes and reduced winter insolation
488 below the Arctic Circle. On an annual average, HTM insolation was higher at high latitudes, but
489 slightly lower in the tropics¹¹³.

490

491 Global-average and high northern-latitude surface temperatures during the HTM appeared to be
492 warmer (at least during summer) than today, while low-latitude climates were slightly cooler¹⁰⁷,
493 consistent with the annual orbital forcing. Although substantial warming was found in the North
494 Atlantic marine sector between 11 and 5 kyr BP¹⁰⁷, recent reconstructions of climate in the mid
495 northern latitudes of continental North America and Europe based on pollen data were characterized

by a cooler HTM with a slow warming as the continental ice sheets retreated¹¹⁴. In contrast, Greenland mean annual atmospheric temperature (after correction for ice sheet altitude changes) peaked earlier, between 10 and 6 kyr BP^{115,116} and was warmer than preindustrial by 1 to 4°C¹¹⁷, while the Nordic seas were only warmer by ~0.5 to 1°C¹¹⁸. The North Pacific Ocean also displayed an early Holocene warming and in most areas a mid-Holocene cooling relative to today, but warming in the North Pacific and East Asia occurred earlier than in the Atlantic sector. Peak warming in the Bering Sea (1-2°C), the western subpolar North Pacific (1-2°C), and the Sea of Okhotsk (2-3°C) occurred between 9 and 11 kyr BP with a possible second warm event between 7 and 5 kyr BP in the Sea of Okhotsk¹¹⁹. In the subpolar NE Pacific off Alaska, peak warming (~1°C above modern, ~3-4°C above mid-Holocene) occurred near 11 kyr BP³³, and in the Pacific off Northern California, peak warmth occurred in two events near 11 kyr BP and again near 10 kyr BP¹²⁰.

In summary, the HTM is a complex regional series of events, best expressed at higher northern latitudes, earliest in the north Pacific marine sector, substantially delayed on land areas influenced by residual ice, and slightly delayed in the North Atlantic and Greenland sector relative to North Pacific and East Asian locations. Although its regional expression makes it difficult to draw a unique global picture, it nevertheless serves as a well-dated and data-rich example of regionally warmer conditions, and is instructive for the impact of warming in these environments. Its complexity also suggests caution in over-interpreting older intervals as being representative of global climate states, because less data are available and chronological constraints are weaker.

The LIG global average sea-surface temperature (SST) was likely 0.5-1°C warmer than preindustrial at least seasonally^{109,121-123} (Table S2). Here we use the value of 0.5±0.3°C as best estimate of the global SST warming at 125 kyr BP¹⁰⁹, a time period when also the northern hemisphere reached a stable warm plateau, although global SST peak warmth may have been somewhat earlier¹²³. Using a

general scaling of global SST to global surface temperature¹⁰³ of 1.6 this implies that global surface temperature was likely ~0.8 (maximum 1.3°C) warmer than preindustrial¹²⁴ and followed a strong orbitally-induced maximum in Northern Hemisphere (NH) summer insolation after a rise in atmospheric CO₂ concentrations from low ice age values to levels only slightly higher than preindustrial (latest data compiled by ref.⁶⁹). Similar to the HTM, significant spatial and temporal differences in the expression of the warming exist; extratropical regions showed more pronounced warming, while tropical regions showed only little warming¹²⁴ or even a slight cooling¹⁰⁹ in line with modeling results¹¹⁰. Temperature reconstructions show a pronounced polar amplification signal in the Arctic during the LIG (see Figure 2), with northern high-latitude oceans warming by >1 to 4°C and surface air temperatures by >3 to 11°C^{46,125,126} relative to preindustrial. As with the HTM, the LIG warming caused by higher northern summer insolation appears to be more representative for regional high-latitude warming than for low latitude warming in the future.

The MPWP was subject to intermittently elevated CO₂ (potentially up to 450 ppm) compared to the HTM and the LIG⁹. The CO₂ concentration at that time was most similar to the RCP2.6 scenario, and a factor of three to four less than concentrations expected by 2100 CE for the RCP8.5 scenario. Climate models simulate an increase in tropical temperatures by 1.0 to 3.1°C (for RCP2.6 CO₂ forcing of 405 ppmv²), generally in line with MPWP proxy reconstructions at low latitudes¹²⁷. Strong polar amplification is observed for the MPWP. For example, proxy data from the North Atlantic and northeastern Russian Arctic indicate a rise of surface air temperatures by 8°C¹²⁸ during the MPWP and even higher in the early Pliocene¹²⁹. These regional temperature changes are similar to projected warming at 2100 AD for the RCP8.5 scenario, in spite of the much lower CO₂ rise during the MPWP, and suggest that current models may underestimate the warming response in the Arctic¹³⁰ to increased CO₂ concentrations.

Box 2 - Constraining climate sensitivity from past warm periods

Fundamental to projecting future warming and impacts is the climate sensitivity to radiative greenhouse forcing, i.e., the global average surface air temperature equilibrium response to a doubling of CO₂. The multi-model mean equilibrium climate sensitivity of the Coupled Model Intercomparison Project Phase 5 (CMIP5) is 3.2°C ± 1.3°C². These models include most of the “fast” feedback processes that result in the “Charney Sensitivity” (CS) but lack some other important processes. In particular, many models do not include some of the real-world “slow” feedback processes relevant for the Earth’s total warming response, such as long-term changes in ice sheets, sea-level, vegetation, or biogeochemical feedbacks that may amplify or reduce the amount of non-CO₂ greenhouse gases in the atmosphere. Furthermore, our understanding of some atmospheric processes under warmer boundary conditions, such as those associated with cloud physics and aerosols, is still limited. The climate models therefore cannot be expected to include realistic long-term feedbacks, which leads to increased uncertainty in climate sensitivity. The long-term climate sensitivity including all these processes is called the Earth System Sensitivity (ESS).

Direct correlation of Pleistocene CO₂ and temperature reconstructions suggest ESS values of 3-5.6 °C^{131,132}. These estimates are based on climate change during glacial cycles. They are therefore indicative of sensitivities associated with large varying glacial ice sheets, and may, therefore, not be appropriate for future warming^{11,133}. When corrected for land-ice albedo feedbacks, vegetation, and aerosols, climate sensitivities implied by these geological estimates may have been 30-40% lower¹³⁴.

We revisit this issue, comparing our paleoclimate data synthesis from episodes warmer than today with published long transient model simulations 10,000 years into the future³ based on a range of CO₂ emission scenarios with two fully coupled climate-carbon-cycle Earth System Models of

Intermediate Complexity (UVic and Bern3D-LPX)³. Both models include fully coupled ocean, atmosphere, sea ice, dynamic vegetation and ocean sediment models with offline ice-sheet models³. Furthermore, we include a published series of equilibrium climate simulations with four dynamic atmosphere-ocean general circulation models, with primitive equation atmospheres (HadCM3L, CCSM3, ECHAM5/MPI-OM, GISS ModelE-R) and one model of intermediate complexity (UVic) under early Eocene boundary conditions^{10,135}.

In Figure B1 we compare global surface air temperature anomalies (relative to preindustrial) to CO₂ (Figure B1a), eustatic sea-level rise relative to CO₂ (Figure B1b), and sea-level rise relative to surface air temperature anomalies (Figure B1c). Paleo data represent the three episodes (HTM, LIG, MPWP) discussed earlier, however, HTM sea-level data are excluded as sea-level is still strongly increasing by deglacial ice sheet melt at that time. To expand the range of climate boundary conditions, we also include data from the EECO (~53-51 Myr BP) when CO₂ was around 1400 ppm and within a possible range of ~900 to 2500 ppm¹³⁶. EECO conditions include changes in the configuration of the continents, land surface topography and albedo changes for loss of continental ice sheets. To separate fast and slow feedbacks, we show EECO model ensemble surface air temperature (SAT) anomalies including all boundary conditions (blue triangles) and values extracting the component related to modified land-surface albedo due to the removal of ice sheets (green squares) in Figure B1a. Model simulations suggest that the loss of ice at the EECO accounts for 0.2 to 1.2°C¹³⁷.

Transient model projections of future warming in response to CO₂ (Figure B1a, black diamonds; see supplementary tables) indicate model ESS of ~3°C, a factor of 2 lower than inferred from the paleo data for the EECO (red squares, see also supplementary tables S1 and S2). EECO model ensemble estimates of warming (after removing the effect of changing surface albedo, green squares) are

594 essentially identical to the transient future runs. The EECO simulations that include the effect of
595 surface albedo (blue triangles) are closer to the paleo reconstructions, but still underestimate the
596 inferred EECO warming at high CO₂, so including interactive land ice as a feedback is essential to
597 reproduce the ESS derived from paleo evidence. This finding echoes previous concern that models
598 built to reproduce present-day climate conditions may be insufficiently sensitive to long-term
599 change⁷.

600
601 For modest CO₂ rises associated with the MPWP, modelled sea level changes are generally
602 consistent with paleo data, but for larger CO₂ rises, the models underestimate the largest sea-level
603 rise such as those reconstructed with larger uncertainties for the EECO (Figure B1b). The UVic
604 model appears to have reasonable sensitivity for the relationship between sea-level rise and warming
605 (Figure B1c, note uncertainty of Eustatic Sea Level (ESL) rise for MPWP). The underestimation of
606 observed past sea level rises by the models is therefore likely due to an underestimation of warming.
607 This misfit becomes important because the rate of sea-level rise in the models is dependent on the
608 extent of warming (Figure B1d). If the models were more sensitive to radiative forcing in particular
609 on long time scales (by up to a factor of two, if they are supposed to fit the paleoclimate data), this
610 would imply a factor of two to three increase in the rate of sea level rise.

611
612 While simulations of climates similar to present day conditions, such as the HTM, agree reasonably
613 well with paleo records, the differences become more substantial for climates that were significantly
614 warmer (MPWP, EECO) but which are also subject to larger uncertainties in temperature and CO₂
615 reconstructions. Climate models underestimate polar amplification (Section 2.1) in the Arctic as well
616 as global mean temperatures and therefore also underestimate the extent and rate of sea-level rise.
617 Hence, climate models are still missing or misrepresenting key processes needed to simulate the
618 dynamics of warmer climates on long time scales. Potential caveats include misrepresentations of

cloud physics and aerosols^{138,139}, ocean and atmosphere circulation changes and insufficient representations of ice sheet and carbon cycle feedbacks.

Although state-of-the-art climate models plausibly have correct sensitivity for small magnitude and near-term projections (such as RCP2.6 at year 2100), they can be questioned to provide reliable projections for large magnitude changes (such as RCP8.5) or long-term climate change (beyond 2100), when Earth System feedbacks become important, and for which the models likely underestimate sensitivity.

631 **References**

- 632 1 Morice, C. P., Kennedy, J. J., Rayner, N. A. & Jones, P. D. Quantifying uncertainties in
633 global and regional temperature change using an ensemble of observational estimates: The
634 HadCRUT4 data set. *J. Geophys. Res. (atmos.)* **117**, n/a-n/a, doi:10.1029/2011jd017187
635 (2012).
- 636 2 IPCC. *Climate change 2013 - the physical science basis*. (Cambridge University Press,
637 2013).
- 638 3 Clark, P. U., Shakun, J. D., Marcott, S. A., Mix, A. C., Eby, M., Kulp, S., Levermann, A.,
639 Milne, G. A., Pfister, P. L., Santer, B. D., Schrag, D. P., Solomon, S., Stocker, T. F., Strauss,
640 B. H., Weaver, A. J., Winkelmann, R., Archer, D., Bard, E., Goldner, A., Lambeck, K.,
641 Pierrehumbert, R. T. & Plattner, G.-K. Consequences of twenty-first-century policy for multi-
642 millennial climate and sea-level change. *Nature Clim. Change* **6**, 360-369,
643 doi:10.1038/nclimate2923 (2016).
- 644 4 Eby, M., Zickfeld, K., Montenegro, A., Archer, D., Meissner, K. J. & Weaver, A. J. Lifetime
645 of anthropogenic climate change: Millennial time scales of potential CO₂ and surface
646 temperature perturbations. *J. Clim.* **22**, 2501-2511, doi:10.1175/2008jcli2554.1 (2009).
- 647 5 Subsidiary Body for Scientific and Technological Advice. Report on the structured expert
648 dialogue on the 2013–2015 review. *United Nations Framework Convention on Climate*
649 *Change* (2015).
- 650 6 Rockström, J., Steffen, W., Noone, K., Persson, Å., Chapin Iii, F. S., Lambin, E. F., Lenton,
651 T. M., Scheffer, M., Folke, C., Schellnhuber, H. J., Nykvist, B., de Wit, C. A., Hughes, T.,
652 van der Leeuw, S., Rodhe, H., Sörlin, S., Snyder, P. K., Costanza, R., Svedin, U.,
653 Falkenmark, M., Karlberg, L., Corell, R. W., Fabry, V. J., Hansen, J., Walker, B., Liverman,
654 D., Richardson, K., Crutzen, P. & Foley, J. A. A safe operating space for humanity. *Nature*
655 **461**, 472, doi:10.1038/461472a (2009).
- 656 7 Valdes, P. Built for stability. *Nat. Geosci.* **4**, 414-416, doi:10.1038/ngeo1200 (2011).
- 657 8 Tzedakis, P. C., Raynaud, D., McManus, J. F., Berger, A., Brovkin, V. & Kiefer, T.
658 Interglacial diversity. *Nat. Geosci.* **2**, 751, doi:10.1038/ngeo660 (2009).
- 659 9 Martinez-Boti, M. A., Foster, G. L., Chalk, T. B., Rohling, E. J., Sexton, P. F., Lunt, D. J.,
660 Pancost, R. D., Badger, M. P. S. & Schmidt, D. N. Plio-Pleistocene climate sensitivity
661 evaluated using high-resolution CO₂ records. *Nature* **518**, 49-54, doi:10.1038/nature14145
662 (2015).
- 663 10 Lunt, D. J., Dunkley Jones, T., Heinemann, M., Huber, M., LeGrande, A., Winguth, A.,
664 Loftson, C., Marotzke, J., Roberts, C. D., Tindall, J., Valdes, P. & Winguth, C. A model–
665 data comparison for a multi-model ensemble of early Eocene atmosphere–ocean simulations:
666 EoMIP. *Clim. Past* **8**, 1717-1736, doi:10.5194/cp-8-1717-2012 (2012).
- 667 11 Paleosens Project Members. Making sense of palaeoclimate sensitivity. *Nature* **491**, 683-691
668 (2012).
- 669 12 Bentley, M. J., Ó Cofaigh, C., Anderson, J. B., Conway, H., Davies, B., Graham, A. G. C.,
670 Hillenbrand, C.-D., Hodgson, D. A., Jamieson, S. S. R., Larter, R. D., Mackintosh, A., Smith,
671 J. A., Verleyen, E., Ackert, R. P., Bart, P. J., Berg, S., Brunstein, D., Canals, M., Colhoun, E.
672 A., Crosta, X., Dickens, W. A., Domack, E., Dowdeswell, J. A., Dunbar, R., Ehrmann, W.,
673 Evans, J., Favier, V., Fink, D., Fogwill, C. J., Glasser, N. F., Gohl, K., Golledge, N. R.,
674 Goodwin, I., Gore, D. B., Greenwood, S. L., Hall, B. L., Hall, K., Hedding, D. W., Hein, A.
675 S., Hocking, E. P., Jakobsson, M., Johnson, J. S., Jomelli, V., Jones, R. S., Klages, J. P.,
676 Kristoffersen, Y., Kuhn, G., Leventer, A., Licht, K., Lilly, K., Lindow, J., Livingstone, S. J.,
677 Massé, G., McGlone, M. S., McKay, R. M., Melles, M., Miura, H., Mulvaney, R., Nel, W.,
678 Nitsche, F. O., O'Brien, P. E., Post, A. L., Roberts, S. J., Saunders, K. M., Selkirk, P. M.,
679 Simms, A. R., Spiegel, C., Stollendorf, T. D., Sugden, D. E., van der Putten, N., van Ommen,

680 T., Verfaillie, D., Vyverman, W., Wagner, B., White, D. A., Witus, A. E. & Zwart, D. A
681 community-based geological reconstruction of Antarctic Ice Sheet deglaciation since the Last
682 Glacial Maximum. *Quat. Sci. Rev.* **100**, 1-9, doi:10.1016/j.quascirev.2014.06.025 (2014).
683 13 Solomina, O. N., Bradley, R. S., Hodgson, D. A., Ivy-Ochs, S., Jomelli, V., Mackintosh, A.
684 N., Nesje, A., Owen, L. A., Wanner, H., Wiles, G. C. & Young, N. E. Holocene glacier
685 fluctuations. *Quat. Sci. Rev.* **111**, 9-34, doi:10.1016/j.quascirev.2014.11.018 (2015).
686 14 Lambeck, K., Rouby, H., Purcell, A., Sun, Y. & Sambridge, M. Sea level and global ice
687 volumes from the Last Glacial Maximum to the Holocene. *Proc. Natl. Acad. Sci.* **111**, 15296-
688 15303, doi:10.1073/pnas.1411762111 (2014).
689 15 Briner, J. P., McKay, N. P., Axford, Y., Bennike, O., Bradley, R. S., de Vernal, A., Fisher,
690 D., Francus, P., Fréchette, B., Gajewski, K., Jennings, A. E., Kaufman, D. S., Miller, G.,
691 Rouston, C. & Wagner, B. Holocene climate change in Arctic Canada and Greenland. *Quat.*
692 *Sci. Rev.* **147**, 340-364 (2016).
693 16 Dutton, A., Carlson, A. E., Long, A. J., Milne, G. A., Clark, P. U., DeConto, R., Horton, B.
694 P., Rahmstorf, S. & Raymo, M. E. Sea-level rise due to polar ice-sheet mass loss during past
695 warm periods. *Science* **349**, doi:10.1126/science.aaa4019 (2015).
696 17 Colville, E. J., Carlson, A. E., Beard, B. L., Hatfield, R. G., Stoner, J. S., Reyes, A. V. &
697 Ullman, D. J. Sr-Nd-Pb isotope evidence for ice-sheet presence on Southern Greenland
698 during the last interglacial. *Science* **333**, 620-623, doi:10.1126/science.1204673 (2011).
699 18 DeConto, R. M. & Pollard, D. Contribution of Antarctica to past and future sea-level rise.
700 *Nature* **531**, 591-597, doi:10.1038/nature17145 (2016).
701 19 Sutter, J., Gierz, P., Grosfeld, K., Thoma, M. & Lohmann, G. Ocean temperature thresholds
702 for Last Interglacial West Antarctic Ice Sheet collapse. *Geophys. Res. Lett.* **43**, 2675-2682,
703 doi:10.1002/2016GL067818 (2016).
704 20 Reyes, A. V., Carlson, A. E., Beard, B. L., Hatfield, R. G., Stoner, J. S., Winsor, K., Welke,
705 B. & Ullman, D. J. South Greenland ice-sheet collapse during Marine Isotope Stage 11.
706 *Nature* **510**, 525-528, doi:10.1038/nature13456 (2014).
707 21 Schaefer, J. M., Finkel, R. C., Balco, G., Alley, R. B., Caffee, M. W., Briner, J. P., Young, N.
708 E., Gow, A. J. & Schwartz, R. Greenland was nearly ice-free for extended periods during the
709 Pleistocene. *Nature* **540**, 252-255, doi:10.1038/nature20146 (2016).
710 22 de Boer, B., Dolan, A. M., Bernales, J., Gasson, E., Goelzer, H., Golledge, N. R., Sutter, J.,
711 Huybrechts, P., Lohmann, G., Rogozhina, I., Abe-Ouchi, A., Saito, F. & van de Wal, R. S.
712 W. Simulating the Antarctic ice sheet in the late-Pliocene warm period: PLISMIP-ANT, an
713 ice-sheet model intercomparison project. *The Cryosphere* **9**, 881-903, doi:10.5194/tc-9-881-
714 2015 (2015).
715 23 Dowsett, H., Dolan, A., Rowley, D., Moucha, R., Forte, A. M., Mitrovica, J. X., Pound, M.,
716 Salzmann, U., Robinson, M., Chandler, M., Foley, K. & Haywood, A. The PRISM4 (mid-
717 Piacenzian) paleoenvironmental reconstruction. *Clim. Past* **12**, 1519-1538, doi:10.5194/cp-
718 12-1519-2016 (2016).
719 24 Naish, T., Powell, R., Levy, R., Wilson, G., Scherer, R., Talarico, F., Krissek, L., Niessen, F.,
720 Pompilio, M., Wilson, T., Carter, L., DeConto, R., Huybers, P., McKay, R. M., Pollard, D.,
721 Ross, J., Winter, D., Barrett, P., Browne, G., Cody, R., Cowan, E., Crampton, J., Dubar, G.,
722 Dunbar, N., Florindo, F., Gebhardt, C., Graham, I., Hannah, M., Hansaraj, D., Harwood, D.,
723 Helling, D., Henrys, S., Hinnov, L., Kuhn, G., Kyle, P., Läufer, A., Maffioli, P., Magens, D.,
724 Mandernack, K., McIntosh, W., Millan, C., Morin, R., Ohneiser, C., Paulsen, T., Persico, D.,
725 Raine, I., Reed, J., Riesselmann, C., Sagnotti, L., Schmitt, D., Sjunneskog, C., Strong, P.,
726 Taviani, M., Vogel, S., Wilch, T. & Williams, T. Obliquity-paced Pliocene West Antarctic ice
727 sheet oscillations. *Nature* **458**, 322-328 (2009).
728 25 Cook, C. P., van de Flierdt, T., Williams, T., Hemming, S. R., Iwai, M., Kobayashi, M.,
729 Jimenez-Espejo, F. J., Escutia, C., González, J. J., Khim, B.-K., McKay, R. M., Passchier, S.,

- Bohaty, S. M., Riesselman, C. R., Tauxe, L., Sugisaki, S., Galindo, A. L., Patterson, M. O., Sangiorgi, F., Pierce, E. L., Brinkhuis, H., Klaus, A., Fehr, A., Bendle, J. A. P., Bijl, P. K., Carr, S. A., Dunbar, R. B., Flores, J. A., Hayden, T. G., Katsuki, K., Kong, G. S., Nakai, M., Olney, M. P., Pekar, S. F., Pross, J., Röhl, U., Sakai, T., Shrivastava, P. K., Stickley, C. E., Tuo, S., Welsh, K. & Yamane, M. Dynamic behaviour of the East Antarctic ice sheet during Pliocene warmth. *Nat. Geosci.* **6**, 765-769, doi:10.1038/ngeo1889 (2013).
- 26 de Vernal, A., Gersonde, R., Goosse, H., Seidenkrantz, M.-S. & Wolff, E. W. Sea ice in the paleoclimate system: the challenge of reconstructing sea ice from proxies – an introduction. *Quat. Sci. Rev.* **79**, 1-8, doi:https://doi.org/10.1016/j.quascirev.2013.08.009 (2013).
- 27 Knies, J., Cabedo-Sanz, P., Belt, S. T., Baranwal, S., Fietz, S. & Rosell-Mele, A. The emergence of modern sea ice cover in the Arctic Ocean. *Nat. Commun.* **5**, 5608, doi:10.1038/ncomms6608 (2014).
- 28 Stein, R., Fahl, K., Gierz, P., Niessen, F. & Lohmann, G. Arctic Ocean sea ice cover during the penultimate glacial and the last interglacial. *Nat. Commun.* **8**, 373, doi:10.1038/s41467-017-00552-1 (2017).
- 29 Spolaor, A., Vallelonga, P., Turetta, C., Maffezzoli, N., Cozzi, G., Gabrieli, J., Barbante, C., Goto-Azuma, K., Saiz-Lopez, A., Cuevas, C. A. & Dahl-Jensen, D. Canadian Arctic sea ice reconstructed from bromine in the Greenland NEEM ice core. *Scientific Reports* **6**, 33925, doi:10.1038/srep33925 (2016).
- 30 Holloway, M. D., Sime, L. C., Allen, C. S., Hillenbrand, C.-D., Bunch, P., Wolff, E. & Valdes, P. J. The Spatial Structure of the 128 ka Antarctic Sea Ice Minimum. *Geophys. Res. Lett.* **44**, 11,129-111,139, doi:10.1002/2017GL074594 (2017).
- 31 Clotten, C., Stein, R., Fahl, K. & De Schepper, S. Seasonal sea ice cover during the warm Pliocene: Evidence from the Iceland Sea (ODP Site 907). *Earth Planet. Sci. Lett.* **481**, 61-72, doi:https://doi.org/10.1016/j.epsl.2017.10.011 (2018).
- 32 Hessler, I., Harrison, S. P., Kucera, M., Waelbroeck, C., Chen, M. T., Anderson, C., de Vernal, A., Fréchette, B., Cloke-Hayes, A., Leduc, G. & Londeix, L. Implication of methodological uncertainties for mid-Holocene sea surface temperature reconstructions. *Clim. Past* **10**, 2237-2252, doi:10.5194/cp-10-2237-2014 (2014).
- 33 Praetorius, S. K., Mix, A. C., Walczak, M. H., Wolhowe, M. D., Addison, J. A. & Prahl, F. G. North Pacific deglacial hypoxic events linked to abrupt ocean warming. *Nature* **527**, 362-366, doi:10.1038/nature15753 (2015).
- 34 Duncan, B., Carter, L., Dunbar, G., Bostock, H., Neil, H., Scott, G., Hayward, B. W. & Sabaa, A. Interglacial/glacial changes in coccolith-rich deposition in the SW Pacific Ocean: An analogue for a warmer world? *Glob. Planet. Chang.* **144**, 252-262, doi:10.1016/j.gloplacha.2016.08.001 (2016).
- 35 Studer, A. S., Sigman, D. M., Martinez-Garcia, A., Benz, V., Winckler, G., Kuhn, G., Esper, O., Lamy, F., Jaccard, S. L., Wacker, L., Oleynik, S., Gersonde, R. & Haug, G. H. Antarctic Zone nutrient conditions during the last two glacial cycles. *Paleoceanography* **30**, 845-862 (2015).
- 36 Jaccard, S. L., Hayes, C. T., Martínez-García, A., Hodell, D. A., Anderson, R. F., Sigman, D. M. & Haug, G. H. Two modes of change in Southern Ocean productivity over the past million years. *Science* **339**, 1419-1423, doi:10.1126/science.1227545 (2013).
- 37 Sigman, D. M., Jaccard, S. L. & Haug, G. H. Polar ocean stratification in a cold climate. *Nature* **428**, 59, doi:10.1038/nature02357 (2004).
- 38 Cane, T., Rohling, E. J., Kemp, A. E. S., Cooke, S. & Pearce, R. B. High-resolution stratigraphic framework for Mediterranean sapropel S5: defining temporal relationships between records of Eemian climate variability. *Palaeogeogr., Palaeoclimatol., Palaeoecol.* **183**, 87-101, doi:https://doi.org/10.1016/S0031-0182(01)00461-8 (2002).

779 39 Kender, S., McClymont, E. L., Elmore, A. C., Emanuele, D., Leng, M. J. & Elderfield, H.
780 Mid Pleistocene foraminiferal mass extinction coupled with phytoplankton evolution. *Nat.*
781 *Commun.* **7**, 11970, doi:10.1038/ncomms11970 (2016).

782 40 Haywood, A. M., Dowsett, H. J. & Dolan, A. M. Integrating geological archives and climate
783 models for the mid-Pliocene warm period. *Nat. Commun.* **7**, 10646,
784 doi:10.1038/ncomms10646 (2016).

785 41 Yasuhara, M., Hunt, G., Breitburg, D., Tsujimoto, A. & Katsuki, K. Human-induced marine
786 ecological degradation: micropaleontological perspectives. *Ecol. Evol.* **2**, 3242-3268,
787 doi:10.1002/ece3.425 (2012).

788 42 Jolly, D., Harrison, S. P., Damnati, B. & Bonnefille, R. Simulated climate and biomes of
789 Africa during the Late Quaternary: Comparison with pollen and lake status data. *Quat. Sci.*
790 *Rev.* **17**, 629-657 (1998).

791 43 Williams, J. W., Shuman, B. & Bartlein, P. J. Rapid responses of the prairie-forest ecotone to
792 early Holocene aridity in mid-continental North America. *Glob. Planet. Chang.* **66**, 195-207,
793 doi:10.1016/j.gloplacha.2008.10.012 (2009).

794 44 Reasoner, M. & Tinner, W. Holocene treeline fluctuations, in *Encyclopedia of*
795 *Paleoclimatology and Ancient Environments* (ed V. Gornitz) 442-446 (Springer, 2008).

796 45 Bigelow, N. H. Climate change and Arctic ecosystems: 1. Vegetation changes north of 55°N
797 between the last glacial maximum, mid-Holocene, and present. *J. Geophys. Res.* **108**,
798 doi:10.1029/2002jd002558 (2003).

799 46 CAPE - Last Interglacial Project Members. Last Interglacial Arctic warmth confirms polar
800 amplification of climate change. *Quat. Sci. Rev.* **25**, 1383-1400,
801 doi:10.1016/j.quascirev.2006.01.033 (2006).

802 47 Larrasoana, J. C., Roberts, A. P. & Rohling, E. J. Dynamics of Green Sahara Periods and
803 Their Role in Hominin Evolution. *PLOS ONE* **8**, e76514, doi:10.1371/journal.pone.0076514
804 (2013).

805 48 de Vernal, A. & Hillaire-Marcel, C. Natural variability of Greenland climate, vegetation, and
806 ice volume during the past million years. *Science* **320**, 1622-1625 (2008).

807 49 Helmens, K. F., Salonen, J. S., Pliik, A., Engels, S., Välranta, M., Kylander, M., Brendryen,
808 J. & Renssen, H. Major cooling intersecting peak Eemian Interglacial warmth in northern
809 Europe. *Quat. Sci. Rev.* **122**, 293-299, doi:10.1016/j.quascirev.2015.05.018 (2015).

810 50 Melles, M., Brigham-Grette, J., Minyuk, P. S., Nowaczyk, N. R., Wennrich, V., DeConto, R.
811 M., Anderson, P. M., Andreev, A. A., Coletti, A., Cook, T. L., Haltia-Hovi, E., Kukkonen,
812 M., Lozhkin, A. V., Rosén, P., Tarasov, P., Vogel, H. & Wagner, B. 2.8 Million Years of
813 Arctic Climate Change from Lake El'gygytgyn, NE Russia. *Science*,
814 doi:10.1126/science.1222135 (2012).

815 51 Urrego, D. H., Sánchez Goñi, M. F., Danialu, A. L., Lechevrel, S. & Hanquiez, V. Increased
816 aridity in southwestern Africa during the warmest periods of the last interglacial. *Clim. Past*
817 **11**, 1417-1431, doi:10.5194/cp-11-1417-2015 (2015).

818 52 Andreev, A. A., Tarasov, P. E., Wennrich, V., Raschke, E., Herzschuh, U., Nowaczyk, N. R.,
819 Brigham-Grette, J. & Melles, M. Late Pliocene and Early Pleistocene vegetation history of
820 northeastern Russian Arctic inferred from the Lake El'gygytgyn pollen record. *Clim. Past* **10**,
821 1017-1039, doi:10.5194/cp-10-1017-2014 (2014).

822 53 Lemoine, D. & Traeger, C. P. Economics of tipping the climate dominoes. *Nat. Clim. Change*
823 **6**, 514-519, doi:10.1038/nclimate2902 (2016).

824 54 Schilt, A., Brook, E. J., Bauska, T. K., Baggenstos, D., Fischer, H., Joos, F., Petrenko, V. V.,
825 Schaefer, H., Schmitt, J., Severinghaus, J. P., Spahni, R. & Stocker, T. F. Isotopic constraints
826 on marine and terrestrial N₂O emissions during the last deglaciation. *Nature* **516**, 234-237,
827 doi:10.1038/nature13971 (2014).

828 55 Marcott, S. A., Bauska, T. K., Buizert, C., Steig, E. J., Rosen, J. L., Cuffey, K. M., Fudge, T.
 829 J., Severinghaus, J. P., Ahn, J., Kalk, M. L., McConnell, J. R., Sowers, T., Taylor, K. C.,
 830 White, J. W. C. & Brook, E. J. Centennial-scale changes in the global carbon cycle during the
 831 last deglaciation. *Nature* **514**, 616-619, doi:10.1038/nature13799 (2014).
 832 56 Rhodes, R. H., Brook, E. J., Chiang, J. C. H., Blunier, T., Maselli, O. J., McConnell, J. R.,
 833 Romanini, D. & Severinghaus, J. P. Enhanced tropical methane production in response to
 834 iceberg discharge in the North Atlantic. *Science* **348**, 1016 (2015).
 835 57 Frank, D. C., Esper, J., Raible, C. C., Büntgen, U., Trouet, V., Stocker, B. & Joos, F.
 836 Ensemble reconstruction constraints on the global carbon cycle sensitivity to climate. *Nature*
 837 **463**, 527-530, doi:10.1038/nature08769 (2010).
 838 58 Bauska, T. K., Joos, F., Mix, A. C., Roth, R., Ahn, J. & Brook, E. J. Links between
 839 atmospheric carbon dioxide, the land carbon reservoir and climate over the past millennium.
 840 *Nat. Geosci.* **8**, 383-387, doi:10.1038/ngeo2422 (2015).
 841 59 Charman, D. J., Beilman, D. W., Blaauw, M., Booth, R. K., Brewer, S., Chambers, F. M.,
 842 Christen, J. A., Gallego-Sala, A., Harrison, S. P., Hughes, P. D. M., Jackson, S. T., Korhola,
 843 A., Mauquoy, D., Mitchell, F. J. G., Prentice, I. C., van der Linden, M., De Vleeschouwer, F.,
 844 Yu, Z. C., Alm, J., Bauer, I. E., Corish, Y. M. C., Garneau, M., Hohl, V., Huang, Y.,
 845 Karofeld, E., Le Roux, G., Loisel, J., Moschen, R., Nichols, J. E., Nieminen, T. M.,
 846 MacDonald, G. M., Phadtare, N. R., Rausch, N., Sillasoo, Ü., Swindles, G. T., Tuittila, E. S.,
 847 Ukonmaanaho, L., Väliranta, M., van Bellen, S., van Geel, B., Vitt, D. H. & Zhao, Y.
 848 Climate-related changes in peatland carbon accumulation during the last millennium.
 849 *Biogeosciences* **10**, 929-944, doi:10.5194/bg-10-929-2013 (2013).
 850 60 Frolking, S. & Roulet, N. T. Holocene radiative forcing impact of northern peatland carbon
 851 accumulation and methane emissions. *Glob. Change Biol.* **13**, 1079-1088,
 852 doi:10.1111/j.1365-2486.2007.01339.x (2007).
 853 61 Stocker, B. D., Yu, Z., Massa, C. & Joos, F. Holocene peatland and ice-core data constraints
 854 on the timing and magnitude of CO₂ emissions from past land use. *Proc. Natl. Acad. Sci.*,
 855 doi:10.1073/pnas.1613889114 (2017).
 856 62 Yu, Z., Loisel, J., Brosseau, D. P., Beilman, D. W. & Hunt, S. J. Global peatland dynamics
 857 since the Last Glacial Maximum. *Geophys. Res. Lett.* **37**, doi:10.1029/2010GL043584,
 858 doi:10.1029/2010GL043584 (2010).
 859 63 Dalton, A. S., Finkelstein, S. A., Barnett, P. J. & Forman, S. L. Constraining the Late
 860 Pleistocene history of the Laurentide Ice Sheet by dating the Missinaibi Formation, Hudson
 861 Bay Lowlands, Canada. *Quat. Sci. Rev.* **146**, 288-299, doi:10.1016/j.quascirev.2016.06.015
 862 (2016).
 863 64 Sierralta, M., Urban, B., Linke, G. & Frechen, M. Middle Pleistocene interglacial peat
 864 deposits from Northern Germany investigated by 230Th/U and palynology: Case studies
 865 from Wedel and Schöningen. *Zeitschrift der Deutschen Gesellschaft für Geowissenschaften*
 866 **168**, 373-387 (2017).
 867 65 Mitchell, W. T., Rybczynski, N., Schröder-Adams, C., Hamilton, P. B., Smith, R. & Douglas,
 868 M. Stratigraphic and Paleoenvironmental Reconstruction of a Mid-Pliocene Fossil Site in the
 869 High Arctic (Ellesmere Island, Nunavut): Evidence of an Ancient Peatland with Beaver
 870 Activity + Online Appendix Figures S1 and S2 (See Article Tools). *Arctic* **69**,
 871 doi:10.14430/arctic4567 (2016).
 872 66 Turetsky, M. R., Benscoter, B., Page, S., Rein, G., van der Werf, G. R. & Watts, A. Global
 873 vulnerability of peatlands to fire and carbon loss. *Nat. Geosci.* **8**, 11-14,
 874 doi:10.1038/ngeo2325 (2015).
 875 67 Hugelius, G., Strauss, J., Zubrzycki, S., Harden, J. W., Schuur, E. A. G., Ping, C. L.,
 876 Schirmer, L., Grosse, G., Michaelson, G. J., Koven, C. D., O'Donnell, J. A., Elberling,
 877 B., Mishra, U., Camill, P., Yu, Z., Palmtag, J. & Kuhry, P. Estimated stocks of circumpolar

878 permafrost carbon with quantified uncertainty ranges and identified data gaps.
879 *Biogeosciences* **11**, 6573-6593, doi:10.5194/bg-11-6573-2014 (2014).

880 68 Bock, M., Schmitt, J., Beck, J. W., Seth, B., Chappellaz, J. & Fischer, H. Glacial/interglacial
881 wetland, biomass burning and geologic methane emissions constrained by dual stable
882 isotopic CH₄ ice core records. *Proc. Natl. Acad. Sci.* **114**, E5778-E5786,
883 doi:10.1073/pnas.1613883114 (2017).

884 69 Bereiter, B., Eggleston, S., Schmitt, J., Nehrbass-Ahles, C., Stocker, T. F., Fischer, H.,
885 Kipfstuhl, J. & Chappellaz, J. Revision of the EPICA Dome C CO₂ record from 800 to 600
886 kyr before present. *Geophys. Res. Lett.* **42**, doi:10.1002/2014GL061957 (2015).

887 70 Loulergue, L., Schilt, A., Spahni, R., Masson-Delmotte, V., Blunier, T., Lemieux, B.,
888 Barnola, J.-M., Raynaud, D., Stocker, T. F. & Chappellaz, J. Orbital and millennial-scale
889 features of atmospheric CH₄ over the past 800,000 years. *Nature* **453**, 383-386 (2008).

890 71 Köhler, P., Knorr, G. & Bard, E. Permafrost thawing as a possible source of abrupt carbon
891 release at the onset of the Bølling/Allerød. *Nat. Commun.* **5**, doi:10.1038/ncomms6520
892 (2014).

893 72 Kennett, J. P., Cannariato, K. G., Hendy, I. L. & Behl, R. J. Carbon isotopic evidence for
894 methane hydrate instability during Quaternary interstadials. *Science* **288**, 128-133 (2000).

895 73 Bock, M., Schmitt, J., Möller, L., Spahni, R., Blunier, T. & Fischer, H. Hydrogen isotopes
896 preclude clathrate CH₄ emissions at the onset of Dansgaard-Oeschger events. *Science* **328**,
897 1686-1689, doi:10.1126/science.1187651 (2010).

898 74 Petrenko, V. V., Smith, A. M., Schaefer, H., Riedel, K., Brook, E., Baggenstos, D., Harth, C.,
899 Hua, Q., Buizert, C., Schilt, A., Fain, X., Mitchell, L., Bauska, T., Orsi, A., Weiss, R. F. &
900 Severinghaus, J. P. Minimal geological methane emissions during the Younger Dryas–
901 Preboreal abrupt warming event. *Nature* **548**, 443-446, doi:10.1038/nature23316 (2017).

902 75 MacDougall, A. H. & Knutti, R. Projecting the release of carbon from permafrost soils using
903 a perturbed parameter ensemble modelling approach. *Biogeosciences* **13**, 2123-2136,
904 doi:10.5194/bg-13-2123-2016 (2016).

905 76 Gregory, J. M. & Huybrechts, P. Ice-sheet contributions to future sea-level change.
906 *Philosophical Transactions of the Royal Society* **354**, 1709-1731 (2006).

907 77 Robinson, A., Calov, R. & Ganopolski, A. Multistability and critical thresholds of the
908 Greenland ice sheet. *Nat. Clim. Change* **2**, 429-432 (2012).

909 78 Hatfield, R. G., Reyes, A. V., Stoner, J. S., Carlson, A. E., Beard, B. L., Winsor, K. & Welke,
910 B. Interglacial responses of the southern Greenland ice sheet over the last 430,000 years
911 determined using particle-size specific magnetic and isotopic tracers. *Earth Planet. Sci. Lett.*
912 **454**, 225-236 (2016).

913 79 Yau, A. M., Bender, M. L., Blunier, T. & Jouzel, J. Setting a chronology for the basal ice at
914 Dye-3 and GRIP: Implications for the long-term stability of the Greenland Ice Sheet. *Earth*
915 *Planet. Sci. Lett.* **451**, 1-9, doi:https://doi.org/10.1016/j.epsl.2016.06.053 (2016).

916 80 Bierman, P. R., Shakun, J. D., Corbett, L. B., Zimmerman, S. R. & Rood, D. H. A persistent
917 and dynamic East Greenland Ice Sheet over the past 7.5 million years. *Nature* **540**, 256-260,
918 doi:10.1038/nature20147 (2016).

919 81 Scherer, R. P., Aldahan, A., Tulaczyk, S., Possnert, G., Engelhardt, H. & Kamb, B.
920 Pleistocene Collapse of the West Antarctic Ice Sheet. *Science* **281**, 82-85,
921 doi:10.1126/science.281.5373.82 (1998).

922 82 Barnes, D. K. A. & Hillenbrand, C.-D. Faunal evidence for a late quaternary trans-Antarctic
923 seaway. *Glob. Change Biol.* **16**, 3297-3303, doi:10.1111/j.1365-2486.2010.02198.x (2010).

924 83 Williams, T., van de Flierdt, T., Hemming, S. R., Chung, E., Roy, M. & Goldstein, S. L.
925 Evidence for iceberg armadas from East Antarctica in the Southern Ocean during the late
926 Miocene and early Pliocene. *Earth Planet. Sci. Lett.* **290**, 351-361,
927 doi:https://doi.org/10.1016/j.epsl.2009.12.031 (2010).

928 84 Golledge, N. R., Levy, R. H., McKay, R. M. & Naish, T. R. East Antarctic ice sheet most
 929 vulnerable to Weddell Sea warming. *Geophys. Res. Lett.* **44**, 2343-2351,
 930 doi:10.1002/2016GL072422 (2017).
 931 85 Steig, E. J., Huybers, K., Singh, H. A., Steiger, N. J., Ding, Q., Frierson, D. M. W., Popp, T.
 932 & White, J. W. C. Influence of West Antarctic Ice Sheet collapse on Antarctic surface
 933 climate. *Geophys. Res. Lett.* **42**, 4862-4868, doi:10.1002/2015gl063861 (2015).
 934 86 Vaughan, D. G., Barnes, D. K. A., Fretwell, P. T. & Bingham, R. G. Potential seaways across
 935 West Antarctica. *Geochem. Geophys.* **12**, n/a-n/a, doi:10.1029/2011GC003688 (2011).
 936 87 Hay, C. C., Morrow, E., Kopp, R. E. & Mitrovica, J. X. Probabilistic reanalysis of twentieth-
 937 century sea-level rise. *Nature* **517**, 481-484, doi:10.1038/nature14093 (2015).
 938 88 Kopp, R. E., Simons, F. J., Mitrovica, J. X., Maloof, A. C. & Oppenheimer, M. A
 939 probabilistic assessment of sea level variations within the last interglacial stage. *Geophysical*
 940 *Journal International* **193**, 711-716, doi:10.1093/gji/ggt029 (2013).
 941 89 O'Leary, M. J., Hearty, P. J., Thompson, W. G., Raymo, M. E., Mitrovica, J. X. & Webster, J.
 942 M. Ice sheet collapse following a prolonged period of stable sea level during the last
 943 interglacial. *Nature Geosci* **6**, 796-800, doi:10.1038/ngeo1890 (2013).
 944 90 Rohling, E. J., Grant, K., Hemleben, C., Siddall, M., Hoogakker, B. A. A., Bolshaw, M. &
 945 Kucera, M. High rates of sea-level rise during the last interglacial period. *Nat. Geosci.* **1**, 38-
 946 42, doi:10.1038/ngeo.2007.28 (2007).
 947 91 Nerem, R. S., Beckley, B. D., Fasullo, J. T., Hamlington, B. D., Masters, D. & Mitchum, G.
 948 T. Climate-change-driven accelerated sea-level rise detected in the altimeter era. *Proc. Natl.*
 949 *Acad. Sci.* **115**, 2022-2025, doi:10.1073/pnas.1717312115 (2018).
 950 92 Tinner, W., Bigler, C., Gedy, S., Gregory-Eaves, I., Jones, R. T., Kaltenrieder, P.,
 951 Krahenbuhl, U. & Hu, F. S. A 700-year paleoecological record of boreal ecosystem responses
 952 to climatic variation from Alaska. *Ecology* **89**, 729-743 (2008).
 953 93 Schwörer, C., Henne, P. D. & Tinner, W. A model-data comparison of Holocene timberline
 954 changes in the Swiss Alps reveals past and future drivers of mountain forest dynamics. *Glob.*
 955 *Change Biol.* **20**, 1512-1526, doi:10.1111/gcb.12456 (2014).
 956 94 Verbesselt, J., Umlauf, N., Hirota, M., Holmgren, M., Van Nes, E. H., Herold, M., Zeileis, A.
 957 & Scheffer, M. Remotely sensed resilience of tropical forests. *Nature Clim. Change* **6**, 1028-
 958 1031, doi:10.1038/nclimate3108 (2016).
 959 95 MacDonald, G. M., Kremenetski, K. V. & Beilman, D. W. Climate change and the northern
 960 Russian treeline zone. *Philos Trans R Soc Lond B Biol Sci* **363**, 2285-2299,
 961 doi:10.1098/rstb.2007.2200 (2008).
 962 96 Scheffer, M., Hirota, M., Holmgren, M., Van Nes, E. H. & Chapin, F. S. Thresholds for
 963 boreal biome transitions. *Proc. Natl. Acad. Sci.* **109**, 21384-21389,
 964 doi:10.1073/pnas.1219844110 (2012).
 965 97 Ruosch, M., Spahni, R., Joos, F., Henne, P. D., van der Knaap, W. O. & Tinner, W. Past and
 966 future evolution of *Abies alba* forests in Europe - comparison of a dynamic vegetation model
 967 with palaeo data and observations. *Glob. Change Biol.* **22**, 727-740, doi:10.1111/gcb.13075
 968 (2016).
 969 98 Colombaroli, D., Tinner, W., Van Leeuwen, J., Noti, R., Vescovi, E., Vanni re, B., Magny,
 970 M., Schmidt, R. & Bugmann, H. Response of broadleaved evergreen Mediterranean forest
 971 vegetation to fire disturbance during the Holocene: insights from the peri-Adriatic region. *J.*
 972 *Biogeogr.* **36**, 314-326, doi:10.1111/j.1365-2699.2008.01987.x (2009).
 973 99 Hirota, M., Holmgren, M., Van Nes, E. H. & Scheffer, M. Global Resilience of Tropical
 974 Forest and Savanna to Critical Transitions. *Science* **334**, 232-235,
 975 doi:10.1126/science.1210657 (2011).
 976 100 Kr pelin, S., Verschuren, D., L zine, A.-M., Eggermont, H., Cocquyt, C., Francus, P., Cazet,
 977 J.-P., Fagot, M., Rumes, B., Russell, J. M., Darius, F., Conley, D. J., Schuster, M., von

978 Suchodoletz, H. & Engstrom, D. R. Climate-Driven Ecosystem Succession in the Sahara: The
 979 Past 6000 Years. *Science* **320**, 765-768, doi:10.1126/science.1154913 (2008).
 980 101 United Nations. The Paris Agreement. *United Nations Treaty Collection* (2015).
 981 102 Ceballos, G., Ehrlich, P. R. & Dirzo, R. Biological annihilation via the ongoing sixth mass
 982 extinction signaled by vertebrate population losses and declines. *Proc. Natl. Acad. Sci.* **114**,
 983 E6089-E6096, doi:10.1073/pnas.1704949114 (2017).
 984 103 Snyder, C. W. Evolution of global temperature over the past two million years. *Nature* **538**,
 985 226-228, doi:10.1038/nature19798 (2016).
 986 104 Hansen, J., Sato, M., Russell, G. & Kharecha, P. Climate sensitivity, sea level and
 987 atmospheric carbon dioxide. *Philosophical Transactions of the Royal Society A* **371**,
 988 doi:10.1098/rsta.2012.0294 (2013).
 989 105 Bartoli, G., Hönisch, B. & Zeebe, R. E. Atmospheric CO₂ decline during the Pliocene
 990 intensification of Northern Hemisphere glaciations. *Paleoceanography* **26**, n/a-n/a,
 991 doi:10.1029/2010PA002055 (2011).
 992 106 Hönisch, B., Hemming, N. G., Archer, D., Siddall, M. & McManus, J. Atmospheric carbon
 993 dioxide concentration across the Mid-Pleistocene Transition. *Science* **324**, 1551-1554 (2009).
 994 107 Marcott, S. A., Shakun, J. D., Clark, P. U. & Mix, A. C. A reconstruction of regional and
 995 global temperature for the past 11,300 years. *Science* **339**, 1198-1201,
 996 doi:10.1126/science.1228026 (2013).
 997 108 PAGES2k Consortium. A global multiproxy database for temperature reconstructions of the
 998 Common Era. *Scientific Reports* **4**, 170088, doi:10.1038/sdata.2017.88 (2017).
 999 109 Hoffman, J. S., Clark, P. U., Parnell, A. C. & He, F. Regional and global sea-surface
 1000 temperatures during the last interglaciation. *Science* **355**, 276-279,
 1001 doi:10.1126/science.aai8464 (2017).
 1002 110 Otto-Bliesner, B. L., Rosenbloom, N., Stone, E. J., McKay, N. P., Lunt, D. J., Brady, E. C. &
 1003 Overpeck, J. T. How warm was the last interglacial? New model–data comparisons.
 1004 *Philosophical Transactions of the Royal Society A* **371**, doi:10.1098/rsta.2013.0097 (2013).
 1005 111 Barber, D. C., Dyke, A., Hillaire-Marcel, C., Jennings, A. E., Andrews, J. T., Kerwin, M. W.,
 1006 Bilodeau, G., McNeely, R., Southon, J., Morehead, M. D. & Gagnon, J. M. Forcing of the
 1007 cold event of 8,200 years ago by catastrophic drainage of Laurentide lakes. *Nature* **400**, 344,
 1008 doi:10.1038/22504 (1999).
 1009 112 Schilt, A., Baumgartner, M., Schwander, J., Buiron, D., Capron, E., Chappellaz, J.,
 1010 Loulergue, L., Schüpbach, S., Spahni, R., Fischer, H. & Stocker, T. F. Atmospheric nitrous
 1011 oxide during the last 140,000 years. *Earth Planet. Sci. Lett.* **300**, 33-43,
 1012 doi:10.1016/j.epsl.2010.09.027 (2010).
 1013 113 Berger, A. & Loutre, M. F. Insolation values for the climate of the last 10 million years.
 1014 *Quat. Sci. Rev.* **10**, 297-317 (1991).
 1015 114 Marsicek, J., Shuman, B. N., Bartlein, P. J., Shafer, S. L. & Brewer, S. Reconciling divergent
 1016 trends and millennial variations in Holocene temperatures. *Nature* **554**, 92,
 1017 doi:10.1038/nature25464 (2018).
 1018 115 Kobashi, T., Menviel, L., Jeltsch-Thömmes, A., Vinther, B. M., Box, J. E., Muscheler, R.,
 1019 Nakaegawa, T., Pfister, P. L., Döring, M., Leuenberger, M., Wanner, H. & Ohmura, A.
 1020 Volcanic influence on centennial to millennial Holocene Greenland temperature change.
 1021 *Scientific Reports* **7**, 1441, doi:10.1038/s41598-017-01451-7 (2017).
 1022 116 Vinther, B., Buchardt, S. L., Clausen, H. B., Dahl-Jensen, D., Johnsen, S., Fisher, D. A.,
 1023 Koerner, R. M., Raynaud, D., Lipenkov, V., Andersen, K. K., Blunier, T., Rasmussen, S. O.,
 1024 Steffensen, J. P. & Svensson, A. M. Holocene thinning of the Greenland ice sheet. *Nature*
 1025 **461**, 385-388, doi:doi:10.1038/nature08355 (2009).

1026 117 Buizert, C., Keisling, B. A., Box, J. E., He, F., Carlson, A. E., Sinclair, G. & DeConto, R. M.
1027 Greenland-Wide Seasonal Temperatures During the Last Deglaciation. *Geophys. Res. Lett.*,
1028 doi:10.1002/2017GL075601 (2018).

1029 118 Eldevik, T., Risebrobakken, B., Bjune, A. E., Andersson, C., Birks, H. J. B., Dokken, T. M.,
1030 Drange, H., Glessmer, M. S., Li, C., Nilsen, J. E. Ø., Otterå, O. H., Richter, K. & Skagseth,
1031 Ø. A brief history of climate – the northern seas from the Last Glacial Maximum to global
1032 warming. *Quat. Sci. Rev.* **106**, 225-246, doi:10.1016/j.quascirev.2014.06.028 (2014).

1033 119 Max, L., Riethdorf, J.-R., Tiedemann, R., Smirnova, M., Lembke-Jene, L., Fahl, K.,
1034 Nürnberg, D., Matul, A. & Mollenhauer, G. Sea surface temperature variability and sea-ice
1035 extent in the subarctic northwest Pacific during the past 15,000 years. *Paleoceanography* **27**,
1036 n/a-n/a, doi:10.1029/2012PA002292 (2012).

1037 120 Barron, J. A., Heusser, L., Herbert, T. & Lyle, M. High-resolution climatic evolution of
1038 coastal northern California during the past 16,000 years. *Paleoceanography* **18**, n/a-n/a,
1039 doi:10.1029/2002PA000768 (2003).

1040 121 Clark, P. U. & Huybers, P. Interglacial and future sea level. *Nature* **462**, 856-857 (2009).

1041 122 McKay, N. P., Overpeck, J. T. & Otto-Bliesner, B. L. The role of ocean thermal expansion in
1042 Last Interglacial sea level rise. *Geophys. Res. Lett.* **38**, n/a-n/a, doi:10.1029/2011GL048280
1043 (2011).

1044 123 CLIMAP project members. The last interglacial ocean. *Quat. Res.* **21**, 123-224 (1984).

1045 124 Turney, C. S. M. & Jones, R. T. Does the Agulhas Current amplify global temperatures
1046 during super-interglacials? *J. Quat. Sci.* **25**, 839-843, doi:10.1002/jqs.1423 (2010).

1047 125 Capron, E., Govin, A., Feng, R., Otto-Bliesner, B. L. & Wolff, E. W. Critical evaluation of
1048 climate syntheses to benchmark CMIP6/PMIP4 127 ka Last Interglacial simulations in the
1049 high-latitude regions. *Quat. Sci. Rev.* **168**, 137-150,
1050 doi:https://doi.org/10.1016/j.quascirev.2017.04.019 (2017).

1051 126 Landais, A., Masson-Delmotte, V., Capron, E., Langebroek, P. M., Bakker, P., Stone, E. J.,
1052 Merz, N., Raible, C. C., Fischer, H., Orsi, A., Prié, F., Vinther, B. & Dahl-Jensen, D. How
1053 warm was Greenland during the last interglacial period? *Clim. Past* **2016**, 1-27,
1054 doi:10.5194/cp-2016-28 (2016).

1055 127 Dowsett, H. J., Robinson, M. M., Haywood, A. M., Hill, D. J., Dolan, A. M., Stoll, D. K.,
1056 Chan, W.-L., Abe-Ouchi, A., Chandler, M. A., Rosenbloom, N. A., Otto-Bliesner, B. L.,
1057 Bragg, F. J., Lunt, D. J., Foley, K. M. & Riesselman, C. R. Assessing confidence in Pliocene
1058 sea surface temperatures to evaluate predictive models. *Nat. Clim. Change* **2**, 365-371,
1059 doi:10.1038/nclimate1455 (2012).

1060 128 Brigham-Grette, J., Melles, M., Minyuk, P. S., Andreev, A. A., Tarasov, P. E., DeConto, R.,
1061 Koenig, S., Nowaczyk, N. R., Wennrich, V., Rosén, P., Haltia-Hovi, E., Cook, T., Gebhardt,
1062 C., Meyer-Jacob, C., Snyder, J. & Herzschuh, U. Pliocene Warmth, Polar Amplification, and
1063 Stepped Pleistocene Cooling Recorded in NE Arctic Russia. *Science* **340**, 1421-1427,
1064 doi:10.1126/science.1233137 (2013).

1065 129 Ballantyne, A. P., Greenwood, D. R., Sinninghe Damsté, J. S., Csank, A. Z., Eberle, J. J. &
1066 Rybczynski, N. Significantly warmer Arctic surface temperatures during the Pliocene
1067 indicated by multiple independent proxies. *Geology* **38**, 603-606, doi:10.1130/g30815.1
1068 (2010).

1069 130 Salzmann, U., Dolan, A. M., Haywood, A. M., Chan, W.-L., Voss, J., Hill, D. J., Abe-Ouchi,
1070 A., Otto-Bliesner, B., Bragg, F. J., Chandler, M. A., Contoux, C., Dowsett, H. J., Jost, A.,
1071 Kamae, Y., Lohmann, G., Lunt, D. J., Pickering, S. J., Pound, M. J., Ramstein, G.,
1072 Rosenbloom, N. A., Sohl, L., Stepanek, C., Ueda, H. & Zhang, Z. Challenges in quantifying
1073 Pliocene terrestrial warming revealed by data–model discord. *Nat. Clim. Change* **3**, 969,
1074 doi:10.1038/nclimate2008 (2013).

- 131 Lea, D. W. The 100 000-Yr Cycle in Tropical SST, Greenhouse Forcing, and Climate
Sensitivity. *J. Clim.* **17**, 2170-2179, doi:10.1175/1520-0442(2004)017<2170:tycits>2.0.co;2
(2004).
- 132 Dyez, K. A. & Ravelo, A. C. Late Pleistocene tropical Pacific temperature sensitivity to
radiative greenhouse gas forcing. *Geology* **41**, 23-26, doi:10.1130/G33425.1 (2013).
- 133 Lunt, D. J., Haywood, A. M., Schmidt, G. A., Salzmann, U., Valdes, P. J. & Dowsett, H. J.
Earth system sensitivity inferred from Pliocene modelling and data. *Nature Geosci* **3**, 60-64
(2010).
- 134 von der Heydt, A. S., Dijkstra, H. A., van de Wal, R. S. W., Caballero, R., Crucifix, M.,
Foster, G. L., Huber, M., Köhler, P., Rohling, E., Valdes, P. J., Ashwin, P., Bathiany, S.,
Berends, T., van Bree, L. G. J., Ditlevsen, P., Ghil, M., Haywood, A. M., Katzav, J.,
Lohmann, G., Lohmann, J., Lucarini, V., Marzocchi, A., Pälike, H., Baroni, I. R., Simon, D.,
Sluijs, A., Stap, L. B., Tantet, A., Viebahn, J. & Ziegler, M. Lessons on climate sensitivity
from past climate changes. *Current Climate Change Reports* **2**, 148-158,
doi:10.1007/s40641-016-0049-3 (2016).
- 135 Meissner, K. J., Bralower, T. J., Alexander, K., Jones, T. D., Sijp, W. & Ward, M. The
Paleocene-Eocene Thermal Maximum: How much carbon is enough? *Paleoceanography* **29**,
946-963, doi:10.1002/2014PA002650 (2014).
- 136 Anagnostou, E., John, E. H., Edgar, K. M., Foster, G. L., Ridgwell, A., Inglis, G. N., Pancost,
R. D., Lunt, D. J. & Pearson, P. N. Changing atmospheric CO₂ concentration was the
primary driver of early Cenozoic climate. *Nature* **533**, 380-384, doi:10.1038/nature17423
(2016).
- 137 Goldner, A., Huber, M. & Caballero, R. Does Antarctic glaciation cool the world? *Clim. Past*
9, 173-189, doi:10.5194/cp-9-173-2013 (2013).
- 138 Kiehl, J. T. & Shields, C. A. Sensitivity of the Palaeocene–Eocene Thermal Maximum
climate to cloud properties. *Philosophical Transactions of the Royal Society A* **371** (2013).
- 139 Sagoo, N., Valdes, P., Flecker, R. & Gregoire, L. J. The Early Eocene equable climate
problem: can perturbations of climate model parameters identify possible solutions?
Philosophical Transactions of the Royal Society A **371** (2013).

1107 **Acknowledgments**

1108 Financial support of the PAGES Warmer World Integrative Activity workshop by the Future Earth
1109 core project PAGES (Past Global Changes) and the Oeschger Centre for Climate Change Research,
1110 University of Bern is gratefully acknowledged. Additional funding by PAGES was provided to the
1111 plioVAR, PALSEA 2, QUIGS, the 2k network, C-peat, Global Paleofire 2 and OC3 PAGES working
1112 groups contributing to in the Integrated Activity (see <http://www.pages.unibe.ch/science/intro> for an
1113 overview of all former and active PAGES working groups). We thank N. Rosenbloom for creating
1114 Figure 2.

1115

1116 **Author Contributions:** The content of this paper is the result of a PAGES workshop taking place in
1117 Bern, Switzerland, in April 2017, which most of the authors attended. All authors contributed to the
1118 literature assessment and the discussion of the results. H.F., K.M. and A.M. developed the concept of
1119 the paper and compiled the paper with support by all coauthors. All coauthors contributed to the
1120 discussion of the manuscript.

1121

1122 **Additional information:**

1123 Supplementary information is available in the [online version of the paper](#). Reprints and
1124 permissions information is available online at www.nature.com/reprints.

1125 Correspondence and requests for materials should be addressed to H.F.

1126

1127 **Competing interests:** The authors declare no competing interests.

1128

1129

Figure Captions

Figure 1 – Changes in global climate and radiative forcing over the last 4 Myr: (a) Changes in

Global Surface Air Temperature (GSAT: Snyder, 2016¹⁰³ (blue line) with 2.5% and 97.5% confidence intervals (light blue shading), Hansen et al., 2013¹⁰⁴ (grey line)) reconstructed from proxy records (left y-axis) and changes in atmospheric CO₂ (right x-axis) from ice core air bubbles (red line: Bereiter et al., 2015⁶⁹) and marine CO₂ proxies (light orange dots: Bartoli et al., 2011¹⁰⁵, dark orange dots: Hönisch et al., 2009¹⁰⁶, green dots: Martinez-Boti et al., 2015⁹) over the last 4 Myr. **(b)** same as in (a) for the last 800,000 years. **(c)** same as in (a-b) for the last 160,000 years. **(d)** GSAT reconstructed from proxy records by Marcott et al. (2013)¹⁰⁷ over the Holocene and the PAGES2k Consortium (2017)¹⁰⁸ together with changes in atmospheric CO₂ from ice core air bubbles (red line⁶⁹). **(e)** Measured GSAT over the last 150 years (HADCRUT4¹) and reconstructed from proxy records over the last 2000 years¹⁰⁸ together with changes in atmospheric CO₂ from ice core air bubbles (red line⁶⁹) and globally averaged atmospheric observations (data from <https://www.esrl.noaa.gov/gmd/>). Note that temperatures in **(d-e)** are given as anomalies relative to the preindustrial mean, where preindustrial is defined as the time interval 1850-1900. Proxy data in **(a-c)** are not available in sufficiently high resolution to unambiguously quantify a mean for this short time interval. Accordingly, (a-c) are given relative to an extended preindustrial reference time interval of the last 1000 years. The horizontal yellow bars indicate the 1.5-2°C warming target relative to preindustrial of the Paris agreement.

Figure 2 – Model-data comparison of climate changes in the future and during the LIG: (a)

RCP2.6 model ensemble (CCSM4) results of Mean Annual Surface Temperature (MAT) anomalies for the time interval 2080–2099 relative to our preindustrial reference interval 1850-1900; **(b)** Observed Last Interglacial (125 kyr BP) annual Sea Surface Temperature (SST) anomalies¹⁰⁹ relative to its reference period 1870-1889 (dots) overlain on top of CCSM3 MAT anomalies for the 125 kyr

1156 BP time window relative to 1850¹¹⁰. White areas in polar areas in panels (a) und (b) represent the
1157 modeled sea ice extent.

1158
1159

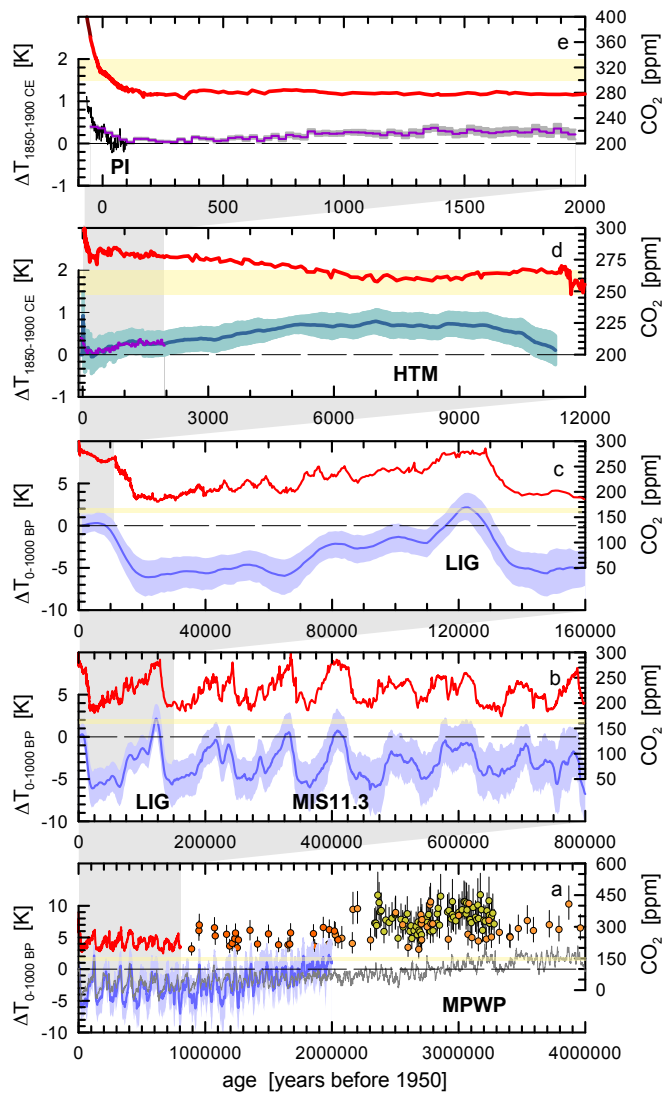
1160 **Figure 3 - Impacts and responses of components of the Earth System:** The figure summarizes the
1161 statements in sections 2 and 3 in extremely condensed form (all statements relative to preindustrial).
1162 Responses where other reasons prohibit a robust statement are given in italic. Additional evidence
1163 that is either not applicable for the future warming or where evidence is not sufficient to draw robust
1164 conclusions is summarized in the supplementary text. Note that significant spatial variability and
1165 uncertainty exist in the assessment of each component and, therefore, this figure should not be
1166 referred to without reading the text in detail.

1167

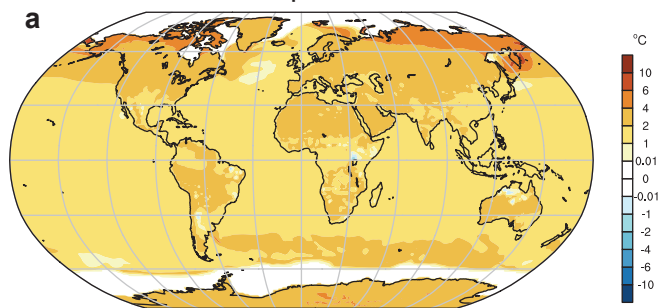
1168 **Figure B1 - Temperature and sea-level response to CO₂ forcing:** (a) Annual and global mean
1169 surface air temperature anomalies (relative to preindustrial) as a function of atmospheric CO₂
1170 concentrations (see supplementary table S1 and S2), (b) eustatic sea-level rise relative to CO₂ levels
1171 (see supplementary table S8 and S10), (c) eustatic sea-level rise relative to surface air temperature
1172 anomalies, and (d) peak rates of eustatic sea-level rise as a function of coeval surface air temperature
1173 anomalies. Black diamonds show simulations of future scenarios by two models of intermediate
1174 complexity³, blue triangles are model ensemble mean equilibrium simulations under EECO
1175 boundary conditions^{10,135}, green squares show EECO simulation responses due to changes in CO₂
1176 concentrations alone, estimated by removing the effects associated with the planetary surface
1177 boundary conditions relative to preindustrial control, and red squares are paleo reconstructions
1178 (supplementary tables S8-S11). Atmospheric CO₂, surface air temperatures and eustatic sea-level
1179 values are averaged over 10,000-12,000 CE in the future simulations (black diamonds, a-c). Peak
1180 rates of simulated sea-level rise occur earlier, between the 23rd and 26th centuries CE, and are
1181 compared to coeval transient model temperatures. The red arrows in b and c indicate minimum

1182 uncertainties. (d). For eustatic sea-levels (b, c) EECO values include melting of the full modern
1183 inventory of ice, plus steric effects (see supplementary Table S10 for details). Changes in ocean
1184 basin shape are excluded from the EECO ESL calculation.

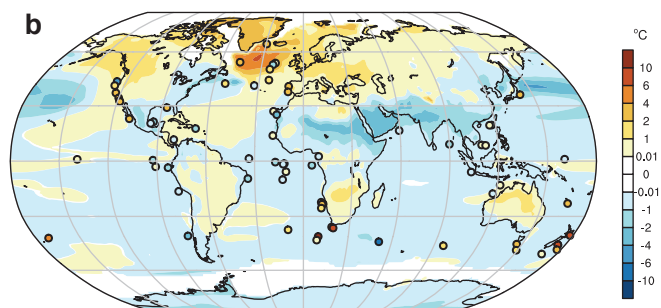
1185



**RCP2.6 annual model SAT anomalies 2080-2099
relative to preindustrial**



**LIG (125 kyr BP) annual model SAT anomalies and
SST reconstructions relative to preindustrial**



Arctic sea ice:

HTM: reduced

LIG: reduced

MPWP: reduced

GIS:

HTM: deglacial reequilibration

LIG: partial retreat

MPWP: smaller

boreal forests:

HTM: northward expansion

LIG: expansion

MPWP: northward expansion

marine ecosystems:

HTM: rather unchanged

LIG: poleward shift

MPWP: poleward shift

Savanna:

HTM: expansion

LIG: expansion likely

MPWP: expansion

marine ecosystems:

HTM: rather unchanged

LIG: poleward shift

MPWP: poleward shift

Antarctic sea ice:

HTM: limited evidence

LIG: reduced

MPWP: reduced

WAIS

HTM: deglacial reequilibration

LIG: partial retreat likely

MPWP: retreat likely

EAIS:

HTM: deglacial reequilibration

LIG: partial retreat possible

MPWP: partial retreat possible

